Free Radical Biology and Medicine xxx (xxxx) 1–13

Contents lists available at ScienceDirect

Free Radical Biology and Medicine

journal homepage: www.elsevier.com/locate/freeradbiomed

New insights in the molecular regulation of the NADPH oxidase 2 activity: Negative modulation by Poldip2

Aicha Bouraoui [a], Ruy Andrade Louzada [b], Sana Aimeur [a], Jehan Waeytens [a, d], Frank Wien [e], Pham My-Chan Dang [c], Tania Bizouarn [a], Corinne Dupuy [b], Laura Baciou [a, *]

[a] Université Paris-Saclay, Institut de Chimie Physique UMR 8000, CNRS, 91405, Orsay Cedex, France
[b] Université Paris Saclay, UMR 9019 CNRS, Gustave Roussy, 94800, Villejuif, France
[c] INSERM U1149, CNRS ERL8252, Centre de Recherche sur l'Inflammation, Université de Paris, Laboratoire d'Excellence Inflamex, Faculté de Médecine, Site Xavier Bichat, Paris, F-75018, France
[d] Structure et Fonction des Membranes Biologiques, Université libre de Bruxelles, Bruxelles, Belgium
[e] Synchrotron SOLEIL, Campus Paris-Saclay, 91192, Gif-sur-Yvette Cedex, France

ARTICLE INFO

Keywords:
Poldip2
NADPH oxidase
Nox2
Nox4
Protein-protein interaction
Reactive oxygen species
Enzyme activity regulation

ABSTRACT

Poldip2 was shown to be involved in oxidative signaling to ensure certain biological functions. It was proposed that, in VSMC, by interaction with the Nox4-associated membrane protein $p22^{phox}$, Poldip2 stimulates the level of reactive oxygen species (ROS) production. In vitro, with fractionated membranes from HEK393 cells over-expressing Nox4, we confirmed the up-regulation of NADPH oxidase 4 activity by the recombinant and purified Poldip2. Besides Nox4, the Nox1, Nox2, or Nox3 isoforms are also established partners of the $p22^{phox}$ protein raising the question of their regulation by Poldip2 and of the effect in cells expressing simultaneously different Nox isoforms. In this study, we have addressed this issue by investigating the potential regulatory role of Poldip2 on NADPH oxidase 2, present in phagocyte cells. Unexpectedly, the effect of Poldip2 on phagocyte NADPH oxidase 2 was opposite to that observed on NADPH oxidase 4. Using membranes from circulating resting neutrophils, the ROS production rate of NADPH oxidase 2 was down-regulated by Poldip2 (2.5-fold). The down-regulation effect could not be correlated to the interaction of Poldip2 with $p22^{phox}$ but rather, to the interaction of Poldip2 with the $p47^{phox}$ protein, one of the regulatory proteins of the phagocyte NADPH oxidase. Our results show that the interaction of Poldip2 with $p47^{phox}$ constitutes a novel regulatory mechanism that can negatively modulate the activity of NADPH oxidase 2 by trapping the so-called "adaptor" subunit of the complex. Poldip2 could act as a tunable switch capable of specifically regulating the activities of NADPH oxidases. This selective regulatory role of Poldip2, positive for Nox4 or negative for Nox2 could orchestrate the level and the type of ROS generated by Nox enzymes in the cells.

Abbreviations

AA	arachidonic acid
BCA	bicinchoninic acid
BSA	bovine serum albumin
CLPX	Caseinolytic Protease X
CP	cytosolic proteins
NADPH	reduced β-nicotinamide adenine dinucleotide phosphate
GST	glutathione-S-transferase
HEK 293	human embryonic kidney 293 cells
PM	plasma membrane
PCNA	*proliferating cell nuclear antigen*
PMSF	phenylmethanesulfonyl fluoride
Poldip2 (PDIP38)	polymerase delta-interacting protein 2
VSMC	vascular smooth muscle cells
YccV	hemimethylated DNA binding protein
PBS	*phosphate-buffered* saline
SOD	superoxide dismutase
MF	membrane fractions

* Corresponding author.
E-mail address: laura.baciou@universite-paris-saclay.fr (L. Baciou).

https://doi.org/10.1016/j.freeradbiomed.2023.02.019
Received 26 December 2022; Received in revised form 6 February 2023; Accepted 21 February 2023
0891-5849/

PRR	proline rich region
SH3	Src homology 3
SDS	sodium dodecyl sulfate
cyt*b*558	cytochrome b_{558}
ECL	enhanced chemiluminescence
ROS	reactive oxygen species
TBST	tris-buffered saline supplemented with 0.1% tween
M-CSF	macrophage colony-stimulating factor
GM-CSF	granulocyte-macrophage colony-stimulating factor
SR-CD	synchrotron radiation circular dichroism
ATR FTIR	attenuated total reflection Fourier transform infrared spectroscopy

1. Introduction

Poldip2 (polymerase delta-interacting protein 2) is also known as PDIP38 [1–4] or mitogenin I [5]. Poldip2 is a soluble 42 kDa (368 amino acids) protein with a mitochondrial addressing sequence that, when cleaved, leads to a 37 kDa protein. Since its discovery in 2003 by Liu et al. from a two-hybrid assay using a human placenta cDNA library [3], studies on this protein have multiplied and have revealed that it is localized in various organs (kidney, heart, aorta, diaphragm, and lung) and cell types where it interacts with a plethora of partners. Different subcellular localization of Poldip2 (cytoplasm, nucleus, mitochondria, or plasma membrane) was described [1,4–6] suggesting that Poldip2 mediates signals by navigating between cellular compartments to transfer information from the cell surface to the genetic machinery [2,5,7].

The mitochondrial signal is important for the interaction of Polidp2 with PrimPol for DNA synthesis in mitochondria [8] but the truncated form of Poldip2, depleted of its mitochondrial signal has been shown to interact with a plethora of proteins through its two protein-protein interacting domains, the N-terminus YccV-like and the C-terminus DUF525 domains [9], as highlighted by the recent structures of Poldip2 showing the ability of these domains to interact with PrimPol, PCNA [10] and CLPX [11]. The YccV-like domain, highly conserved in eukaryotes, is found in particular in the HspQ (Heat shock protein Q) protein and is also involved in the binding of hemimethylated DNA and the regulation of *dna*A gene expression [12–14]. The DUF525 domain of the Poldip2 protein was found from sequence analyses to share homology with the bacterial ApaG protein (30% sequence identity) [3] and the C-terminal part of some proteins of F-box protein family well known as protein-protein interacting proteins [15,16].

By interacting with many different partners, Poldip2 was shown to be involved in the regulation of various biological functions [9,17]. On one hand, Poldip2 appeared to have beneficial functions such as in DNA replication, damage response and repair [3,4,8,18,19], ATP, peptide hormones, and neuropeptides biosynthesis [1,20,21], and cell adhesion [22,23] [6,24,25]. Poldip2 has been also described as playing a crucial role in Tau aggregation [26]. On another hand cellular functions, Poldip2 has been associated with diverse diseases such as cardiac pathologies [27], and breast and lung cancer diseases [28–32] and was shown to be involved in chemo-resistance [33]. By regulating mitochondrial lipoylation, Poldip2 allows cancer cells to adapt to hypoxic conditions in their new environment [34]. Poldip2 deficiency protects against lung oedema and vascular inflammation in a model of acute respiratory distress syndrome and was shown to be involved in the regulation of vascular barrier (blood-brain barrier) [35] and attenuated the infiltration of myeloid cells, inflammatory monocytes/macrophages via unknown mechanisms [36] and brain blood permeability [37].

Finally, Poldip2 was also shown to be involved in oxidative signaling. It was described that, by stimulating reactive oxygen species (ROS) production, Poldip2 positively regulates neurodegenerative diseases [38]and cerebral ischemia [9]. In the kidney, the Poldip2-induced increased production of ROS activates different signaling pathways in the renal cells to ensure certain biological functions of this organ, including diuresis [39] and the formation of fibroblasts [40,41]. In VSMC, it was demonstrated that Poldip2 induces an increased ROS production [6], with downstream effects on cytoskeletal changes required for cell migration [22,23].

In mammals, NADPH oxidases are one of the major sources of ROS in cells. The NADPH oxidase (Nox) family consists of seven catalytic subunits named Nox1-5, Duox1, and 2 (for Dual oxidase) [42]. They are membrane-bound proteins containing the NADPH binding site and redox carriers (two hemes and one flavin) for transferring electrons through the membrane to dioxygen to generate ROS. Nox1, Nox2, Nox3, and Nox5 produce superoxide anions ($O_2^{\bullet-}$), precursors of more highly reactive species like hydrogen peroxide (H_2O_2), $HO^{\bullet}$, and HOCl. Nox4 and Duox produce mostly H_2O_2 with minimal production of superoxide [43]. These enzymes are expressed in diverse cells and tissues, and their products are required for several physiological roles like host defense, hormone synthesis, cell proliferation, vascular, cell signaling, and regulation of gene expression. Dysregulation of their activity can lead to oxidative stress-related aging, carcinogenesis, and neurodegenerative and immune diseases.

Nox1, Nox2, Nox3, and Nox4 isoforms require a membrane-bound subunit, $p22^{phox}$. The membrane protein 22^{phox} is considered a "maturation factor" involved in complete biosynthesis of Nox isoforms and essential for their maturation and structural stability. Among these Nox, Nox4 is constitutively active [44] and does not require subunits other than $p22^{phox}$ to be functional [45]. Only Poldip2 has been shown to upregulate Nox4 by interacting with $p22^{phox}$ [6]. The activation of the other $p22^{phox}$ depending Nox (Nox1, Nox2, and Nox3) isoforms is dependent on the translocation of additional cytosolic subunits.

The quasi-ubiquitous presence of Poldip2 and its navigation between cellular compartments result in possible co-localization of Poldip2 with isoforms other than Nox4 and notably those associated with $p22^{phox}$ (Nox1, Nox2, Nox3). Lyle's group showed that Poldip2 co-localized with Nox1 in VSMC but without observing any regulatory effect of Poldip2 on this enzyme. The numerous tissue co-localization of NADPH oxidase 4 and 2 [39,46–50], or subcellular co-localization, i.e. the endoplasmic reticulum (ER) [51] raises the issue of a possible effect of cross-regulation between Nox4 and Nox2 isoforms. Moreover, co-expression of Poldip2 and Nox2/$p22^{phox}$ was described at the level of renal arterioles [52,53], and very recently it was also described in neutrophils during the hematopoietic differentiation [25]. However, to date, no data are available on a possible regulatory effect of Poldip2 on the activity of NADPH oxidase 2 (Nox2) which is the most efficient ROS-generating isoform in cells, in particular in phagocytes, including neutrophils and monocytes. Therefore, in this report, we explored whether Poldip2 could act as a novel regulatory protein of the Nox2. To this purpose, a functional recombinant Poldip2 was produced and purified. Its interaction with the different protein components of the Nox2 complex, on the one hand, the membrane components, Nox2/$p22^{phox}$ (forming the so-called cytochrome b_{558} in phagocytic cells), and on the other hand the cytosolic regulatory proteins, $p47^{phox}$, $p67^{phox}$, and the small G protein of the Rho family (Rac1-2), has been explored. Poldip2 preferred partners have been identified and the subsequent effect on the Nox2 activity was investigated.

2. Materials and methods

2.1. Cloning of Poldip2 cDNA and yeast transfection

The plasmid KLCF-N containing rat Poldip2 cDNA was kindly given by Pr. B. Lassègue and was used to amplify the cDNA by PCR using the forward [CAT CCG CGG TAA GGC TGG TTG TGT GGC C] and reverse

[CGC GTC TAG AGC CCA GTG AAG GCC TGA GGG TG] oligonucleotide primers. The PCR product was digested with SacII and XbaI and inserted into the *P. pastoris* expression vector pPICZαA. The Poldip2 cDNA was inserted downstream of the promoter of the alcohol oxidase I gene (AOX1), the α-factor secretion signal from *Saccharomyces cerevisiae,* and upstream of 6xhis- and cmyc-tags. The resulting plasmid, pPICZαA/Poldip2-his-cmyc (Fig. S1), was used to transform *E.coli* Top10 competent cells. Transformants were selected on zeocin (100 μg/mL) LB agar plates. The plasmid was extracted from *E. coli* and sequenced.

2.2. Poldip2 expression in Pichia pastoris

Empty pPICZαA and pPICZαA/Poldip2-His-cmyc vectors were linearized with Pme*I* restriction enzyme and used to transform *P. pastoris* SMD1168 and X-33 strains by electroporation following manufacturer instructions (Invitrogen). Positive clones were selected on YPD agar (1% yeast extract, 2% peptone, 2% dextran) supplemented with appropriate antibiotic (1 mg/mL zeocin). The selected clone was grown overnight in 5 mL of BMGY (1% yeast extract, 2% peptone, 100 mM potassium phosphate, pH 6.0, 1.34% yeast nitrogen base with amino sulfate, 4.10^{-5}% biotin, 1% glycerol, 100 μg/mL zeocine) at 30 °C. 2 mL from the yeast culture was added to 250 mL of BMGY supplemented with zeocin (100 μg/mL). After 48 h of culture, cells were harvested and resuspended in 1 L of BMMY without zeocin. Cells were grown in a baffled culture flask at 25 °C with shaking at 180 rpm for 72 h. Methanol (0.5% v/v final concentration) was added every 24 h to maintain protein expression. The culture was centrifuged at 4000 rpm for 20 min and the supernatant was used immediately for purification and protein analysis.

2.3. Poldip2 purification

One liter of culture supernatant was loaded on a column of Ni-Excel Sepharose™ (Cytiva). The column was washed with 25 mM sodium phosphate pH 7.4; 500 mM NaCl, 50 mM imidazole, and recombinant protein was eluted with the same buffer supplemented with 300 mM of imidazole. The recombinant protein was concentrated using rotavapor (Heidolph Hei-VAP advantage) and dialyzed against 20 mM sodium phosphate pH 7.4, 150 mM NaCl, 10 mM $MgSO_4$. The purity of the protein was analyzed by Coomassie blue stained SDS PAGE (12%) and the protein was quantified by bicinchoninic acid assay (BCA) or Nanodrop technique. For immunoblot analyses, the gels were transferred to a nitrocellulose membrane (Cytiva). The membranes were incubated overnight at 4 °C with specific monoclonal or polyclonal antibodies: anti-gp91 (anti-$gp91^{phox}$; 54.1; mouse monoclonal, dilution 1:1500; Santa Cruz), anti-p22 (44.1; mouse monoclonal; dilution 1:1500; Santa Cruz); anti-Poldip2 (ab181841; rabbit monoclonal; , dilution 1:1500; Abcam), anti-p67 (07-002; rabbit polyclonal; dilution 1:1000; Millipore); Anti-p47 (BD 610354; rabbit polyclonal; dilution 1:1500; Bioscience), anti-Rac1 (ARCO3; mouse monoclonal; dilution 1:500; Cytoskeleton), anti-NOX4 (ab109225; rabbit monoclonal; dilution 1:1500; Abcam). The immune complex was detected with either goat anti-rabbit (dilution 1:15000; Santa Cruz) or goat anti-mouse (dilution 1:15000; Santa Cruz) secondary antibodies conjugated to peroxidase. The bound peroxidase activity was detected by an imaging system (PXi, Syngene) using ECL reagents (ECL West Pico Amersham®). The experiments were performed at least three times independently, unless noted in the legend, with similar results.

2.4. Human neutrophil and monocyte isolation

Monocytes and neutrophils were isolated from the human blood of healthy donors obtained at the Etablissement Français du Sang (EFS, Paris, France, agreement numbers n°2022-2026-003 and 13/NECKER/094). For accurate comparison between neutrophils, monocytes, and macrophages, blood from the same donor was used each time. About 400 mL blood was mixed to an equal volume of 2% dextran solution, diluted in 0.9% NaCl solution, and set for sedimentation for 30 to 45 min. The supernatant was centrifuged for 8 min at 400 × *g* to harvest the leucocytes. Pellets were resuspended in a 50 mL final volume of PBS. Neutrophils were separated from monocytes and lymphocytes in Ficoll solution for 30 min at 400 × *g*. The mono-lymphocytes ring was gently collected and set for further separation. The pellet containing neutrophils was re-suspended in PBS and the red cells were lysed by osmotic shock with 0.6 M KCl solution for 40 s. The broken red cells were then eliminated by centrifugation (8 min at 400 × *g*). The neutrophil pellet was resuspended in cold buffer containing 20 mM phosphate pH 7.4, 340 mM Sucrose, 7 mM $MgSO_4$, 200 μM leupeptin, and 1 mM PMSF (breaking buffer) for further step of the neutrophil membrane preparation.

The mono-lymphocyte ring was washed with PBS containing 0.5% BSA and 1 mM EDTA then diluted to a final concentration of 5 $.10^7$ cells/mL in the same buffer. The monocytes were purified using the EasySep™ Human Monocyte Enrichment kit according to the manufacturer's instructions.

2.5. Human monocyte differentiation into macrophages

5 $.10^6$ Monocytes isolated from human blood donors were seeded into 6 wells plate in RPMI medium containing 10% SVF penicillin and streptomycin. In tissues, monocytes can differentiate into generally two populations of macrophages: on the one hand, classically activated M1 macrophages, known to be pro-inflammatory and bactericidal, and, on the other hand, alternately activated M2 macrophages, known to be anti-inflammatory. In vitro, monocytes were differentiated into M1 and M2 type macrophages by adding the differentiation factors GM-CSF and M-CSF, respectively. M-CSF and GM-CSF differentiation factors were added at a final concentration of 50 ng/mL. Cells were cultured for 6 days at 37 °C at 5% CO_2. The isolated cells were lysed using an isotonic buffer containing 100 mM Tris HCl pH7, 2.5% SDS, 1 mM EDTA, 1 mM EGTA, 4 M Urea, 1 mM PMSF, and 10 μg/mL leupeptin, pepstatin and aprotinin. The extracts were analyzed by Western blot.

2.6. Neutrophil membrane preparation

Neutrophils cells were sonicated in breaking buffer containing 20 mM phosphate pH 7.4, 340 mM sucrose, 7 mM $MgSO_4$,200 μM leupeptin, and 1 mM PMSF using the 30% pulse mode at power pulse 3 in an ice-cooled beaker 12 times during 10 s with an interval of 1 min between sonication [54]. The cell lysate was centrifuged for 15 min at 10.000 × *g*, the supernatant was then centrifuged for 1 h 45 min at 240000 × *g*. The pellet containing the membrane fraction was solubilized in breaking buffer, aliquoted, and stored at −80 °C.

The cytb_{558} (Nox2 or $gp91^{phox}$/$p22^{phox}$) concentration in neutrophil membranes was quantified as described in Ref. [54]. Briefly 1% dodecyl maltoside was added to solubilize membrane fraction from neutrophils. Sodium dithionite-reduced *minus* oxidized difference absorption spectra were recorded at room temperature using an Uvikon dual-beam spectrophotometer between 400 and 600 nm. The cytb_{558} concentration was calculated from difference absorption at 427 nm and 411 nm using the extinction coefficient of 200 mM^{-1} cm^{-1}.

Human cytosolic proteins (p47phox, p67phox, and Rac) were expressed in Escherichia coli BL21 (DE3) using pET15b-Hisp67*phox*, pET15b-Hisp47*phox*, pGEX2T-GST-Rac1Q61L vectors provided by Dr. Dagher (IBS, Grenoble, France). Purification chromatography including SP-Sepharose Fast-Flow (FF), Q-Sepharose-FF, Glutathione Sepharose-FF, and Ni-NTA-Sepharose-FF resins (Cityva, France) was carried out using ÄKTAprime system as described in Ref. [54]. The protein purity was determined by SDS gel (10% bis-trisNupage, Biorad) using Coomassie brilliant blue.

2.7. Dot blot binding assays

The dot blot hybridization was used to determine the binding capacity of Poldip2 to bind or not to the cytosolic proteins. Different amounts of recombinant $p47^{phox}$ (5–64 pmol), $p67^{phox}$ (4–49 pmol), and Rac (5–62 pmol) proteins were coated on a nitrocellulose membrane (0.2 μm pore size; Amersham). The membrane was then blocked with 2.5% BSA/TBST and washed three times in TBST for 10 min. The membranes were then incubated with a solution containing 100 nM Poldip2 and 0.5% BSA/TBST. The membrane was again washed three times in TBST for 10 min and labeled with an antibody raised against Poldip2 followed by a secondary antibody coupled to peroxidase (1:15000). Reactive spots were revealed by chemiluminescence (ECL West Pico Amersham®). Dotblot intensities were quantified by using ImageJ software. Graph pad prism 5 software was utilized for data analysis to determine the *K*d value for Poldip2 and $p47^{phox}$ interaction. To validate this technique to quantify protein-protein interaction, the same procedure was used to determine the *K*d value for $p47^{phox}$ and $p67^{phox}$ interaction, except that $p67^{phox}$ (5–64 pmol) was coated and incubation was done with 100 nM $p47^{phox}$ revealed with an antibody raised against $p47^{phox}$ was used. The experiments were performed twice with similar results. Values were corrected for background signal.

2.8. Measurement of NADPH oxidase activity using cell-free assays

Neutrophil membrane fractions (4 nM cytb_{558}) were mixed with the cytosolic proteins ($p47^{phox}$, $p67^{phox}$, and Rac1Q61L, 300 nM each) in PBS solution in a spectrophotometer cuvette. When mentioned, incubation in the presence of arachidonic acid (32 μM) for 5 min at 25 °C was performed. The total volume of the solution was 600 μL. The activities measurements were performed by monitoring the NADPH (200 μM) consumption rates at 340 nm (or the equivalent of μmol of $O_2^{\bullet-}$/sec for the specific activity of the NADPH oxidase) which showed to be a more accurate approach for the vesicular context of NADPH oxidase activity measurements [55]. The *Cis*-Arachidonic acid (AA) was purchased from Sigma-Aldrich, France, and NADPH from ACROS, France. Data are mean ± SEM of 3 or more independent experiments.

2.9. Membrane co-sedimentation experiments

The membrane fractions from neutrophils were incubated for 1 h with the recombinant Poldip2 with a cytb_{558}:Poldip2 ratio of 1:20 (mol:mol) or as described in the figure legends. The mix is then centrifuged at 190.000 × *g* for 1 h to pellet the membrane fraction keeping the soluble proteins in the supernatant. As a control, the same procedure was performed for the protein Poldip2 and neutrophil membrane fractions alone.

2.10. HEK 293 cell line cultures, cell fractioning, and ROS measurements

HEK 293 cells, derived from human embryonic kidney cells, stably overexpressing NOX4 upon tetracycline induction, kindly given by Karl-Heinz Krause (Geneva, Switzerland [45]) were cultured in 100 mm plates in DMEM medium containing 4.5 g/L glucose 10% TET-free SVF, 1 mM sodium pyruvate, 2 mM L-alanyl-L-glutamine (GlutaMAX™-I), 100 U/mL penicillin, 100 μg/mL streptomycin and 400 μg/mL G418. When cells reached 80% of confluence, doxycycline was added at a final concentration of 10^{-2} μg/mL and the cells were cultured for 12 h to induce NOX4 expression. HEK 293 cells were also cultured without doxycycline as a control. HEK 293 cells, were harvested from 100 mm plates and re-suspended in 50 mM de sodium phosphate pH 7 containing 1 mM EGTA, 2 mM $MgCl_2$, 1 mM PMSF and supplemented with protease inhibitor. Cells were broken using a Dounce homogenizer. Cell lysate was centrifuged for 5 min at 500 × *g* to isolate the nucleus. The supernatant was centrifuged at 12000 × *g* for 15 min to isolate the mitochondria/endoplasmic reticulum (ER) fraction. Finally, the enriched plasma membrane fraction was isolated by centrifugation of the supernatant at 200000 × *g* for 45 min. All cell fractions were resuspended in 50 mM sodium phosphate at pH 7.0, containing 2 mM $MgCl_2$, 250 mM sucrose, 1 mM PMSF, protease, and phosphatase inhibitor cocktails (Roche). The subcellular fractions isolated from HEK cell (30 μg) were incubated in 50 m*M* sodium phosphate buffer (pH 7.2) containing sucrose (250 m*M*), EGTA (1 m*M*), $MgCl_2$ (2 m*M*) and in presence of Poldip2 at a final concentration of 183 nM or 367 nM or 550 nM. Just before adding 0.2 m*M* NADPH to start the reaction, SOD (200 U/mL), horseradish peroxidase (0.25 U/mL), and amplex red (50 μ*M*) were added to the solution. Fluorescence was measured immediately in a microplate reader (Victor3; PerkinElmer) at 30 °C for 30 min using excitation at 571 nm and emission at 585 nm. H_2O_2 release was quantified in nanomoles of H_2O_2per min per mg of total protein using standard calibration curves.

2.11. 3D model building of the rat Poldip2 structure

The automated protein structure homology-modeling server, SWISS-MODEL [56] was used to generate the 3D model of rat Poldip2. Molecular modeling was analyzed based on the X-ray crystallographic structure of the human Poldip2 (Ref PDB: 6Z9C).

The Alpha Fold modeling of the complex Poldip2-$p47^{phox}$ was performed using the Alphafold2-advanced that was run on google Collaboratory computing facilities [57]. Google colab was run using default parameters. All structural images were generated using PyMol Software molecular graphics system (Schrödinger; www.pymol.org).

2.12. Circular dichroism spectroscopy

Synchrotron radiation circular dichroism (SRCD) spectra were collected on the DISCO beamline at the synchrotron radiation SOLEIL, Gif-sur-Yvette, France. All spectra were calibrated in respect of wavelengths and amplitudes with camphor sulphonic acid (CSA). Samples were loaded in CaF_2 cells containing 25 μL volumes and optical pathlengths of 33 and 50 μm depending on the protein concentrations (between 14 and 40 μM).

Spectra were measured from 280 to 170 nm, using the mid-height of the HT (high tension) as cut-off at 175 nm. Three consecutive scans were recorded and averaged for the samples and the baseline. The averaged baseline was subtracted from the averaged sample spectra and smoothed with 7 points using the Savitsky-Golay algorithm. The temperature was kept constant at 25 °C.

Spectra are expressed in delta epsilon units, calculated using mean residue weight. The secondary structure composition was determined using the software BeStSel (https://bestsel.elte.hu/index.php).

2.13. ATR FTIR (attenuated total reflection; fourier transform InfraRed) spectroscopy

Spectra were obtained with the Bruker Equinox 55 instrument. The spectrometer is continuously purged with dry air. 2 μL of the sample are deposited on a diamond crystal and dried with a light nitrogen flow. 128 scans are recorded between 4000 cm^{-1} and 800 cm^{-1} for both the sample and the blank (buffer). The secondary structures are determined from the specific bands at amide I (1700-1620 cm^{-1}) and amide II (1600-1510 cm^{-1}) by applying the calibration developed previously by Goormaghtigh et al. [58].

2.14. Statistical analysis

Statistical analysis was performed using GraphPad Prism 5.0. Data are represented as the mean ± standard error of the mean (SEM). Significance was determined using Student's *t*-test or Repeated Measures

ANOVA (and non-parametric). A p-value of ≤0.05 was considered statistically significant.

3. Results

3.1. Expression, purification, and characterization of recombinant Poldip2

The rat *Poldip2* gene shares a very high identity with humans (95%), mice (99%), and bovine (95%) (Fig. 1A). The highest percentage of variable residues is present in the mitochondrial targeting signal of Poldip2 leading to the mature Poldip2 protein, conserved between rat and human except for two residues V86A and S240 N. Heterologous rat Poldip2 was produced in the heterologous *Pichia pastoris* expression system (SMD1168 strain). Yeast is currently widely used as an expression system performing post-translational changes such as phosphorylation. Our previous attempt to produce rat Poldip2 intracellularly was unsuccessful, likely due to toxicity for yeast. Therefore, the rat *Poldip2* gene was cloned into the pPICZαA expression vector that contains the α-factor signal sequence for protein secretion (Fig. S1). The secretion pathway shows the advantage of the purification procedure because only a few endogenous proteins are secreted by yeast in the culture media. Clones with the gene inserted into the yeast genomic DNA by cross-linking were selected based on the level of expression of the recombinant Poldip2. After purification of the extracellular media on Nickel-Excel affinity chromatography, the two lower bands were recognized by antibodies raised against Poldip2 (Fig. 1B). The antibody His-tag recognition demonstrated the integrity of the C-terminus of the purified proteins and a probably truncated N-terminus (Fig. 1B).

Mass spectrometry (MS) analysis of the tryptic digest of the three SDS-PAGE gel bands confirmed the non-reliability of the highest band to Poldip2 whereas it unfailingly identified Poldip2 with 80% and 37% sequence coverage for the two lower bands (Fig. S2). The protein molecular weights were estimated to be 39 and 29 kDa, respectively on SICaPS platform (Service d'Identification et de Caractérisation des Protéines par Spectrométrie de masse), by measuring the m/z (mass-to-charge) ratio of their gas-phase ions for the mass spectrometry analysis. Consistent with Western blot analysis, both proteins were found to be N-terminally truncated, lacking the mitochondrial targeting signal: the 39 kDa (the majoritarian form) and 29 kDa forms of Poldip2 were truncated from residue 1 to 54 ($Poldip2_{55\text{-}368}$) and from residue 1 to 129 ($Poldip2_{130\text{-}368}$), respectively. In addition, mass spectrometry did not detect any phosphorylation of Poldip2.

The structural analyses of purified Poldip2 estimated from the SR-CD and ATR FTIR spectra (Fig. S3) are gathered in Table 1. Both spectroscopies suggest that Polidp2 is composed of a small number of α-helixes (*ca.* 4–7%), a higher percentage of β-sheets (15–23%), and turns (15–22%), and a high amount of unordered secondary structure (>

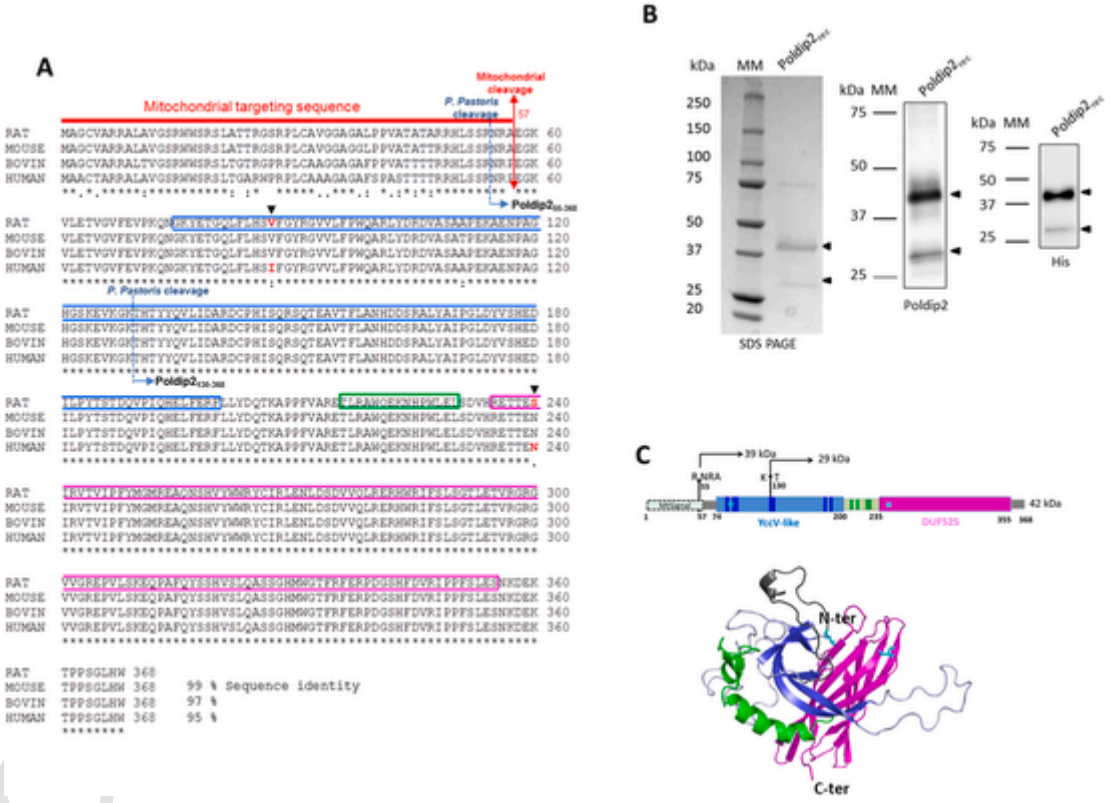

Fig. 1. A. Comparison of the Poldip2 protein sequences from rat, bovine, mouse and human species. Not conserved residues are indicated in red. The mitochondrial targeting signal sequence is mentioned by a red line with the cleavage designed by a red arrow. The non-specific cleavage occurred in the yeast secretion pathway is indicated with blue arrows; The non-conserved amino acids between rat and human (Val86 in the YccV domain and Ser240 in the DUF525 domain) are colored in red. The YccV and DUF525 domains are boxed in blue and magenta, respectively. In green is boxed the α-helix present in the linker region. **B. Purified Poldip2 by Nickel affinity chromatography.** Purified Poldip2 analysis by Coomassie blue SDS-PAGE. Western Blot analysis using an antibody raised against Poldip2 (1:1500). Western Blot analysis using an antibody raised against the histidine tag (1:500). 10 μg and 5 μg of purified Poldip2 was loaded respectively for SDS-PAGE and Western Blot analysis. MM: molecular marker. This biochemical study was performed many times independently (>10 times) with similar results; **C. Sequence scheme and structural model of rat Poldip2**. The structural model of the 39 kDa Poldip2 was obtained by Swiss modeling software. The YccV like domain (residue 74–200) is colored in light blue where the 5 antiparallel β-strands are indicated with dark blue boxes in the scheme. The DUF525 domain (residue 235–355) is shown in magenta. The non-conserved amino acids between rat and human (Val86 in the YccV domain and Ser240 in the DUF525 domain) are colored in cyan in the structural model and as stars in the scheme. The linker region (light green) between both domains is organized in α-helix and two β-strands (indicated with dark green boxes in the scheme). (For interpretation of the references to color in this figure legend, the reader is referred to the Web version of this article.)

Table 1
SR-CD and Infrared spectra analysis of purified Poldip2. Experimental data (Fig. S3) were analyzed using BeStSel and Matlab software, respectively. The results are given as a percentage (±15%).

	α-helixes (%)	β-sheets (%)	Turn (%)	Others (%)
SR-CD	4.6	23.1	15.5	56.8
IR	7	15	22	56

56%). This SR-CD analysis is consistent with the high β-strand content CD spectra obtained for human Poldip2 [10].

Using the SWISS-MODEL program, we determined a model structure of rat Poldip2 (Fig. 1C) based on the recent crystallographic structure of human Poldip2 at 2.8 Å resolution [10]. The resulting structure model of rat Poldip2 was superimposable with the human Poldip2 structures (PDB code 6Z9C and 6ZLX; see Fig. S4). In the model, the structure of rat Poldip2 recovered the overall organization described in human Poldip2 with the N-terminal YccV and the C-terminal DUF525 domains. The YccV-like domain (residues 74–200) is organized in five antiparallel β-strands of the SH3-type domain similar to the structural organization of the HspQ (Heat shock protein Q) protein [52]. The DUF525 domain (residues 235–368) comprises four-antiparallel β strands (immunoglobulin-like fold) reminiscent of bacterial ApaG and eukaryote FBox proteins) [7,59] and is preceded by a helical alpha helix (residues 216–234). In the two recent X-ray structures of human Poldip2 [10,11], two disordered regions (105–126 and 136–170) were not solved. In our structure model obtained using Swiss-model software, these regions are described as two flanking disordered wings of the YccV-like domain, consistent with the structure model of rat Poldip2 that we have obtained from alphafold software [60]. The two non-conserved amino acids between human and rat proteins (V86A and S240 N; Fig. S4) are located on the surface of the protein and, according to our model, do not affect protein folding.

3.2. Effect of recombinant rat Poldip2 on the activity of human NADPH oxidase 4

To verify whether the purified recombinant Poldip2 (the majority form Poldip2$_{55\text{-}368}$ (39 kDa) cleaved 3 amino acids upstream of the mitochondrial cleavage site) was functional in terms of its ability to upregulate NADPH oxidase 4 activity [6], we used membrane fraction isolated from HEK 293 cell line. HEK 293 cells express endogenously human Nox4 and p22^{phox}. To increase the Nox4 expression level in these cells, they were transfected with a vector harboring the human Nox4 coding gene under the control of doxycycline treatment. Doxycycline-treated and -untreated cells were harvested and broken. The mitochondria/ER and plasma membrane subcellular compartments were separated and enriched by differential centrifugation and analyzed by western blots (data not shown). The mitochondria/ER and plasma membrane subcellular fractions isolated from doxycycline-treated and non-treated cells were used to determine the effect of the extemporaneous addition of purified recombinant Poldip2 on ROS production rates by NADPH oxidase 4 (Fig. 2).

Without the addition of Poldip2 to both subcellular membrane fractions, hydrogen peroxide productions are low but not zero corresponding to the constitutive activity of NADPH oxidase 4. After Poldip2 addition, H_2O_2 production rates increased as a function of Poldip2 concentration. The most important effect of Poldip2 on NADPH oxidase activity is observed in the mitochondria/ER from doxycycline-treated cells where H_2O_2 production rates increased two-fold from 50 to 100 nmol $H_2O_2.s^{-1}.mg^{-1}$, values close to what were observed in VSMC cells [6]. Although a slight increase in H_2O_2 production rates was measured with both treated and untreated plasma membrane fractions as the concentration of Poldip2 increased, it is interesting to note that these H_2O_2 production rates are much less strong plasma membrane fractions than with mitochondria/ER membranes. The importance of the membrane environment on oxidase activity is not unexpected. The fact that the composition of the plasma membrane, being different from that of the mitochondria or ER, would not allow Poldip2 to potentiate the activity of the Nox4-based NADPH oxidase. Such difference in NADPH oxidase activity depending on its subcellular location was previously reported by Kuroka and coll [61]. Moreover, our group has demonstrated the similar importance of the ER membrane environment compared to plasma membranes on NADPH oxidase 2 activity [62].

The main objective of these experiments was to verify the functionality of the recombinant Poldip2 protein. Our results showed that recombinant and purified Poldip2 positively regulated in vitro the activity of NADPH oxidase 4 present in membrane fractions from HEK293 cell lines to a similar extent as described with VSMC cells, confirming that the recombinant protein is functional. Furthermore, these results show that this can occur in a cross-species manner since the upregulation of human NADPH oxidase 4 by rat Polidp2.

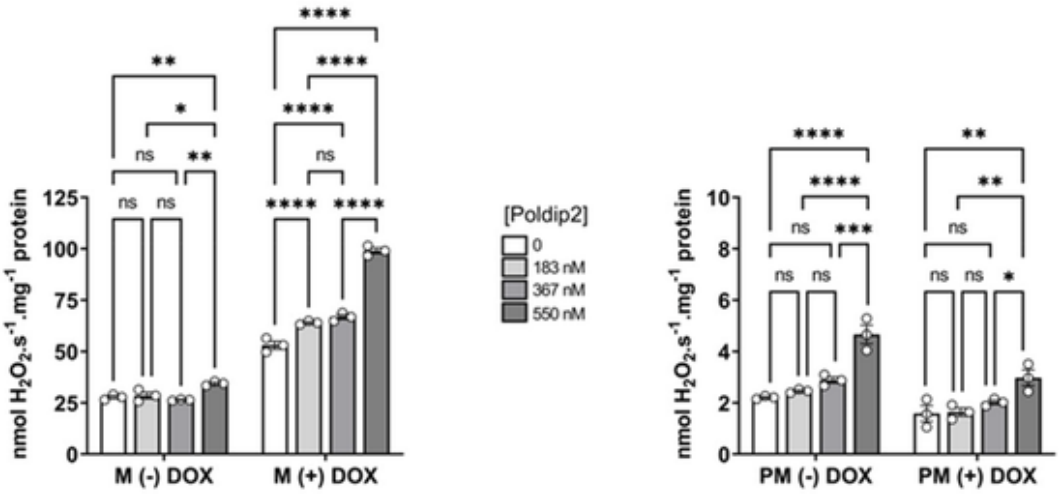

Fig. 2. Upregulation of human NADPH oxidase 4 by rat Poldip2. The effect of addition of increased concentration of recombinant Poldip2 on the activity of the NADPH oxidase 4 was measured using mitochondria and plasma membrane fractions from HEK 293 cell line stably transfected with Nox4 coding gene. The H_2O_2 production rates were measured as described in Materials and Methods using the amplex red HRP method detection. (−) cells without doxycycline treatment; (+) cells treated with 10^{-2} μg/mL of doxycycline for 12 h. M: mitochondria; PM: Plasma membrane. *P < 0.05, **P < 0.01, ***P < 0.001 and ****P < 0.0001. These measurements were performed in triplicate for two independent experiments. The results are expressed as means ± SEM.

3.3. Poldip2 effect on phagocyte NADPH oxidase activity

To investigate the effect of Poldip2 on the activity of phagocyte NADPH oxidase 2, we compared the presence of endogenous Poldip2 in white blood cells isolated from healthy donors. Monocytes and neutrophils were isolated from the same healthy donor blood. Monocytes were differentiated into M1 (pro-inflammatory and bactericidal) and M2 (anti-inflammatory) macrophages. The presence of Poldip2, Nox2 (gp91^{phox}), and p22^{phox} was investigated in the different cells. As expected, significant levels of gp91^{phox} (glycosylated) and p22^{phox} were found in neutrophils and differentiated macrophages and a smaller amount in monocytes (Fig. 3, ponceau staining in Fig. S5). Interestingly, Poldip2 was identified in macrophages and monocytes but not in circulating neutrophils. Due to the absence of detected Poldip2 in isolated circulating neutrophils, these cells were considered the best models for this study and were used to prepare membrane fractions (MF) containing cytb_{558} (gp91^{phox}/p22^{phox}).

The activity of NADPH oxidase 2 was determined using the canonical cell-free assay procedure [63,64]. Classically, it consists in mixing neutrophil membrane fractions (MF) with equimolar concentration of p47^{phox}, p67^{phox}, and Rac (CP; for cytosolic proteins) in the presence of an activator, arachidonic acid (AA). The superoxide production rate is monitored by the NADPH consumption at 340 nm (or equivalent in mol of $O_2^{\bullet-}$). In the control experiment, the NADPH oxidase activation by the translocation of the cytosolic proteins to gp91^{phox}/p22^{phox} is optimal and the superoxide production rate is very high (Fig. 4). In the absence of the cytosolic proteins and of AA, or when Poldip2 has incubated alone with the neutrophil MF, no ROS production was measured (data not shown).

Unexpectedly, the addition of Poldip2 to this canonical cell-free assays lead to a decreased superoxide production rate (Fig. 4). This superoxide production rate decreases with increasing Poldip2 concentration, up to a factor of 2.5. The effect of Poldip2 on gp91^{phox}/p22^{phox} is the opposite of the effect on NOX4/p22^{phox} for which an increase in ROS production was observed. This suggests different mechanisms. The decreased activity of gp91^{phox}/p22^{phox} in the presence of Poldip2 might be explained by an impairment of either activation or assembly processes of the NADPH oxidase 2 complex or both.

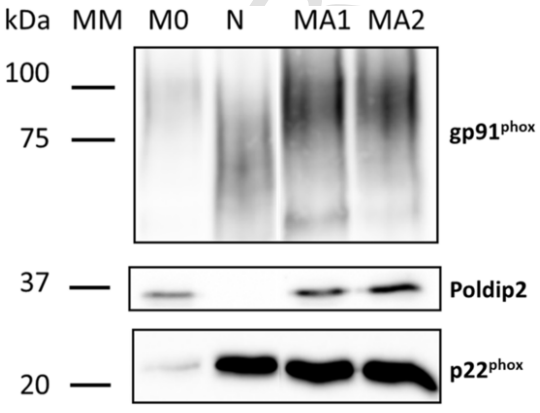

Fig. 3. Comparison of gp91^{phox}, Poldip2 and p22^{phox} expression in monocytes, neutrophils and macrophages isolated from healthy donor blood. M0: monocyte; N: neutrophil; MA1 and MA2 macrophage type 1 (pro-inflammatory and anti-tumoral) and 2 (pro-tumoral and anti-inflammatory). 12 μg of total protein (cell lysates) are loaded. The ponceau staining of these western blots is shown in Fig. S5. All samples are from the same donor. Experiment was repeated independently twice with similar results for blood from two healthy donors.

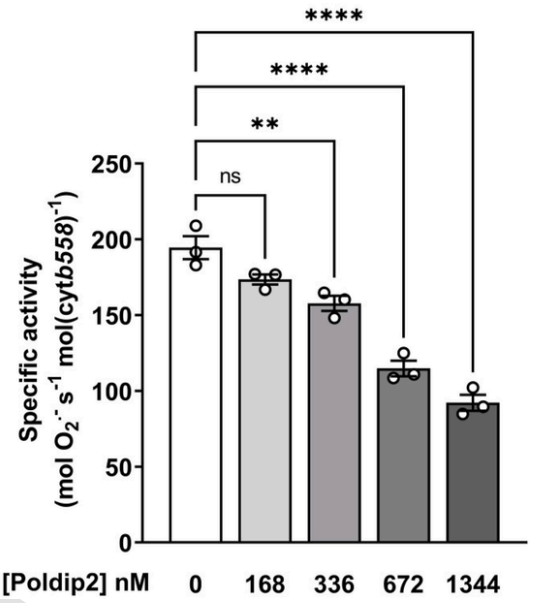

Fig. 4. Effect of Poldip2 on the activity of NADPH oxidase 2. The activities measurements were performed by monitoring the NADPH (200 μM) consumption rates at 340 nm (or equivalent of μmol of $O_2^{\bullet-}$/sec). The kinetics of NADPH consumption was followed for the different samples. The canonical cell-free assay includes neutrophil membrane fraction containing the cytb_{558} (4 nM) in the presence of CP (Cytosolic Proteins containing p67^{phox}, p47^{phox}, Rac1Q61L, ≈300 nM each and arachidonic acid (32 μM); To this canonical cell free assay, increased amount of Poldip2 was added together with CP. *P < 0.05, **P < 0.01, ***P < 0.001 and ****P < 0.0001. Data are mean ± SEM of 3 measurements. Experiments were performed in triplicate with similar results with blood from two different healthy donors.

3.4. Interaction of Poldip2 with neutrophil membrane fractions

Poldip2 was demonstrated to associate with p22^{phox} to activate NADPH oxidase 4 [6]. To test the hypothesis of the association of Poldip2 with p22^{phox} associated with gp91^{phox}, we mixed neutrophil membranes containing gp91^{phox}/p22^{phox} with purified Poldip2. After incubation, the mix was ultra-centrifuged. Then, the pellets and supernatants were analyzed by western blots (Fig. 5). The revelation of the western blots with anti- Nox2 antibodies showed that as expected, gp91^{phox} was detected in the ultracentrifugation pellet containing the neutrophil MF, with only traces remaining in the supernatant. Poldip2 being a soluble protein was found, as expected, in the supernatant. When Poldip2 was incubated with the neutrophil MF, Poldip2 was this time revealed in the pellet too, although the signal was found very weak. This demonstrates that Poldip2 can co-sedimented with the ultracentrifugation pellet in the presence of MF. Using different ratios of cytb_{558}/Poldip2, we observed that Poldip2 interaction with the membrane increased when the cytb_{558}/Poldip2 ratio was higher suggesting that Poldip2 interaction with MF in neutrophils might be cytb_{558} concentration-dependent (data not shown).

3.5. Partner identification of Poldip2

To identify whether the down-regulation of gp91^{phox}/p22^{phox} by Poldip2 occurred by interaction with the membrane fraction or with the cytosolic proteins, Poldip2 (336 nM) was incubated first either with the neutrophil membrane fraction or the soluble regulatory proteins p47^{phox}, p67^{phox} and Rac), prior the cell-free assay measurements (Fig. 6).

When Poldip2 and the neutrophil membranes were incubated first together and then mixed with the cytosolic proteins incubated separately with AA, no significant change in the measured ROS production

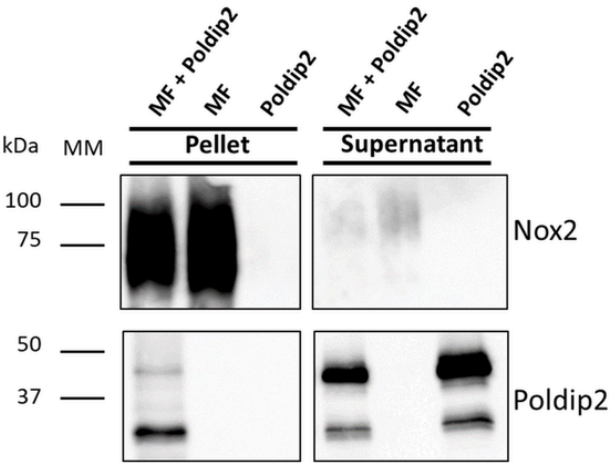

Fig. 5. Poldip2 interaction with purified membrane fraction isolated from human neutrophils. Poldip2 (145 µl; 0.2 µM) and neutrophil membrane fractions (MF; 1.75 µl; 1.28 µM), containing the cytb_{558} (gp91^{phox}/p22^{phox}), were pre-incubated for 1 h with the cytb_{558}/Poldip2 ratio of 1:20 (mol:mol). The MF and Polidp2 (alone) were treated similarly. The three samples were centrifuged at 190 000 × *g* for 1h30. Pellet and supernatant were separated and analyzed by Western blot using antibodies raised against Nox2 (1:1500), p22^{phox} (1:1500) and Poldip2 (1:1500). Experiments were performed at least three times with similar results.

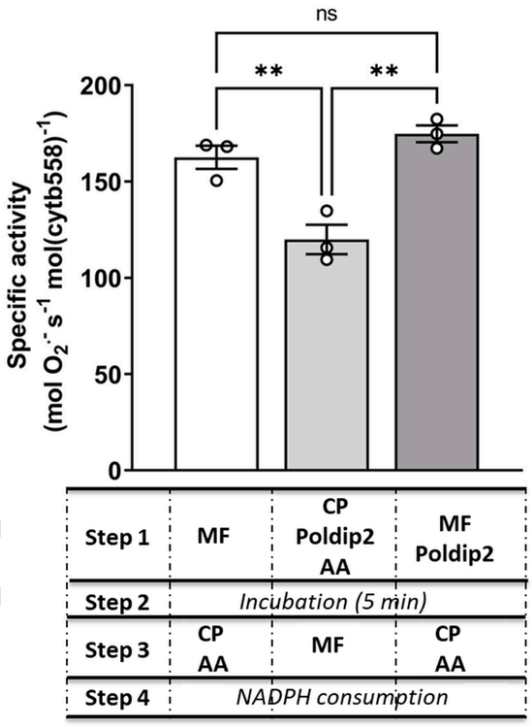

Fig. 6. Effect of Poldip2 on activity of NADPH oxidase 2 according to the sequence of its introduction into the cell free assay mixture. Poldip2 was mixed with either the cytosolic proteins in the presence of AA (light grey) or the membrane fraction (dark grey). An incubation of 5 min was preformed (25 °C) before the addition of the membrane fraction and cytosolic proteins with AA, respectively. The enzyme activity was then immediately measured by monitoring the NADPH consumption at 340 nm. The canonical cell-free assay was used as control (white barrel). MF: neutrophil membrane fraction; 4 nM cytb_{558}; CP: Cytosolic proteins containing p67^{phox}, p47^{phox}, Rac1Q61L, 300 nM each with arachidonic acid (32 µM); Poldip2 (336 nM). *P < 0.05, **P < 0.01, ***P < 0.001 and ****P < 0.0001. Data are mean ± SEM of 3 independent experiments.

rates was observed compared to the canonical cell-free assay where MF, cytosolic proteins, and AA were incubated together in the absence of Poldip2. Although Poldip2 slightly interacts with the membrane component as described above, this interaction was not responsible for the down-regulation of the enzyme activity. Interestingly no further inhibition (expected to be of about 20% according to Fig. 4) was observed due to the mostly unbound Poldip2 to the membrane by the time the cytosolic proteins were added. This indicates that Poldip2 was not able to interact with the activated (AA-incubated) cytosolic proteins [54,65]. In contrast, when Poldip2 and the cytosolic proteins were first incubated in the presence of AA prior to mixing with the MF, a significant inhibition of NADPH oxidase activity was observed compared to the canonical cell-free assay. This suggests that the co-presence of Poldip2 with the non-activated cytosolic proteins alters the ROS production rates of the enzyme.

These results show that Poldip2 interferes with the assembly of the oxidase complex by preventing the interaction of at least one of the cytosolic proteins (p47^{phox}, p67^{phox}, or Rac) with their membrane partners.

Direct binding evidence was obtained by performing dot blot-binding assays using recombinant proteins. Different amounts of recombinant target proteins (p47^{phox}, p67^{phox}, and Rac) were applied onto nitrocellulose (0.2 µm pore size) membranes. After blocking and washing, the membranes were incubated with recombinant Poldip2. After extensive washing, the dot blots were incubated with antibodies directed against Poldip2. Reactive spots were revealed using chemiluminescence. The results are shown in Fig. 7A and B. A very strong signal for p47^{phox} was detected, in contrast to p67^{phox} and Rac. The chemiluminescence signal increased as a function of the amount of p47^{phox} deposited, indicating that there is a functional interaction between the two proteins. This result showed that Poldip2 strongly interacts with the p47^{phox} subunit.

Analysis of the individual spots allowed using a one-to-one binding model to semi-quantitatively determine an apparent dissociation constant value (*Kd*) of 3.08 ± 0.8 µM for the interaction between p47^{phox} and Poldip2 (Fig. 7E). To validate this semi-quantitative method for *Kd* determination, we used the same method to estimate the already known *Kd* value for p67^{phox}-p47^{phox} [66–68]. This time, increased concentrations of recombinant p67^{phox} were coated on the membrane blot and after incubation with p47^{phox}, the bound p47^{phox} to p67^{phox} was revealed using an antibody raised against p47^{phox} (Fig. S6). Using the one-to-one model, the quantification of the individual spots leads to the apparent *Kd* value of the interaction on blots between p47^{phox} and p67^{phox} of about 0.8 ± 0.4 µM (Fig. 7F). Although this value is slightly high compared to the *Kd* values obtained in solution (≈0.15–0.04 µM), it remains sufficiently in the range to consider the semi-quantitative method applicable for comparative studies. The apparent affinity of Poldip2 and p47^{phox} is about 3.8 fold smaller than the affinity between p67^{phox} and p47^{phox}. Consistent with this, the dot blotted mixture of p67^{phox} and p47^{phox} showed reduced Poldip2 intensity compared to the intensity on the dot blot of p47^{phox} alone. This indicate that p67phox compete with poldip2 for p47phox binding (Fig. 7C). In unstimulated phagocyte cells the interaction between p67^{phox} and p47^{phox} is known to occur between the C-terminal PRR region of p47^{phox} and the SH3 domain of p67^{phox} [69,70]. To check if the C-terminal PRR region of p47^{phox} could be the region involved in the interaction with Poldip2, dot blot hybridization was performed with the PRR region-truncated p47^{phox} (1–134 amino acids) (Fig. 7D). The dot blot showed no signal of Poldip2 interaction with the truncated p47^{phox} compared with the full length p47^{phox} suggesting that the C-terminal region (PRR region) of p47^{phox} is likely the common binding target of either Poldip2 or p67^{phox}.

Overall, our data show that Poldip2 interferes with the complex assembly inducing an alteration of the production of ROS. This occurs via the interaction of Podip2 with p47^{phox}, the adaptor protein of p67^{phox} to bind gp91^{phox} and p22^{phox}. The protein-protein interactions remain to

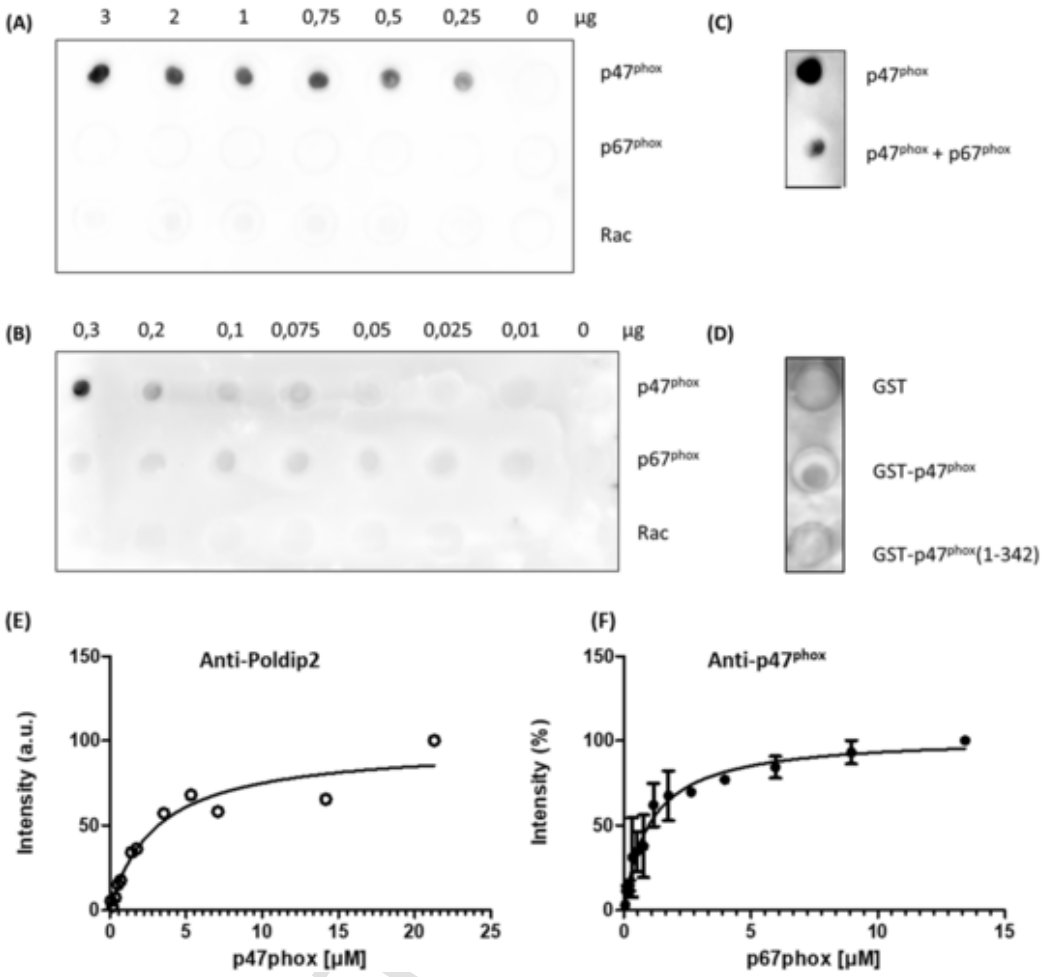

Fig. 7. Poldip2 interaction with cytosolic proteins p47^{phox}, p67^{phox} and Rac. A dilution series of p47^{phox}, p67^{phox} and Rac proteins were spotted on the nitrocellulose membrane. After incubation with 100 nM Poldip2, the membrane was incubated with antibody raised against Poldip2. Lighter dots correspond to lower amount of Poldip2 bound to the protein target. **(A)** p47^{phox} (5–64 pmol), p67^{phox} (4–49 pmol) and Rac (5–62 pmol). Experiment was repeated independently twice with similar results**. (B)** p47^{phox} and Rac (0,2–5 pmol) p67^{phox} (0,16 - 4 pmol). A and B could be fitted using GraphPad with a model of specific binding **(E) (C)** Dot blot hybridization of Poldip2 was performed with p47^{phox} or with p47^{phox}/p67^{phox} (20 pmol of p47^{phox} and 16 pmol of p67^{phox}). Experiments were repeated independently twice with similar results. **(D)** Dot blot hybridization of Poldip2 with full-length p47^{phox} (1–390) and with p47^{phox} (1–342) truncated from its C-terminus PRR region; 20 pmol of GST, GST-p47 and GST-p47ΔCter. Glutathione S-transferase (GST) was used as negative control. **(F)** Fitting of dot blot hybridization of p47^{phox} with p67^{phox} (Fig. S4) using GraphPad with a model of specific binding.

be clarified. The PRR region of p47^{phox}, involved in an interaction with p67^{phox} is a good candidate for the Poldip2 interacting region (Fig. 8).

4. Discussion

The possible co-localization of the NADPH oxidase2 and 4 with Poldip2 in several cell types raises crucial questions about their cross regulation. This issue is based on the fact that Nox2 and Nox4 proteins have the same partner p22^{phox}, which has been proposed as the protein interacting with Poldip2 in the case of Nox4-based NADPH oxidase. Although the mechanism of regulation of Nox4 activity by Poldip2 has not been identified, the authors hypothesized that Poldip2 would, by stabilizing the Nox4-p22^{phox} complex, lead to an up-regulation of ROS production [6]. In this work, we aimed to investigate the role of Poldip2 on NADPH oxidase 2 at the molecular level using phagocyte cell membranes. For this purpose, we have produced Poldip2 (rat) in a yeast expression system and purified it. Recombinant Poldip2 (39 29 kDa being the majority form) was truncated at their N-terminus from the mitochondrial targeting signal sequence. Our SR-CD and IR analyses let us conclude that rat Poldip2 structure with about 6.9% of α –helixes, 37% of β-sheets and a high amount of disordered secondary structures. Our structural models of the rat Poldip2 showed a globular protein that comprises two domains: the (SH3-type) YccV-like and DUF525 domains similar to the 3D structures obtained recently for human Poldip2 [10,11].

The function of the purified rat Poldip2 was investigated by measuring its effect on ROS production in HEK293 cells expressing human Nox4 and p22^{phox}. The observed increased ROS production (>2-fold) close to the up-regulation measured for Nox4-based NADPH oxidase activity in VSMC by a factor of 3 [6], confirmed the functionality of the purified Poldip2. Moreover, it underlined that a cross-species regulation by Poldip2 was possible. Once these preliminary controls were validated the purified Poldip2 was used to study at the molecular level whether and how Poldip2 can modulate the Nox2-based NADPH oxidase.

4.1. Effect of Poldip2 on the activity of the NADPH oxidase 2

Poldip2, alone, cannot replace the known regulatory subunits p47^{phox}, p67^{phox}, and Rac(1/2) to activate gp91^{phox}/p22^{phox} (data not shown). When introduced into the complex assembly process, we demonstrated that Poldip2 inhibits substantially the activity of NADPH oxidase 2. This decreased activity was unexpected considering that the

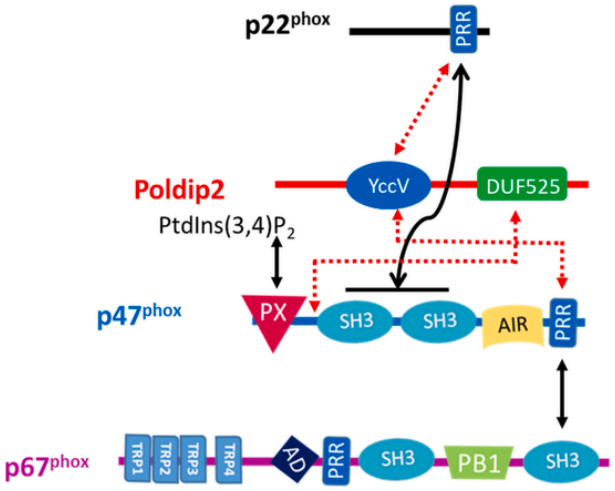

Fig. 8. Scheme of domains of NADPH oxidase partners involving Poldip2. The central role of p47^{phox} is highlighted for its protein-protein and lipid-protein interactions indicated with black arrows for NADPH oxidase 2 activity. p47^{phox} through its bis-SH3 domains interacts with the PRR region of p22^{phox}. The PRR region of C-terminus p47^{phox} interacts with the SH3 domain of p67^{phox} and its PX domain interacts with phosphoinositides of the membrane. The negative regulatory role of Poldip2 on NADPH oxidase 2 activity would occur as a result of the interaction of Poldip2 with p47^{phox} preventing the latter from interacting with p67^{phox} to translocate it and form the active NADPH oxidase complex. The putative interactions of Poldip2 are indicated with dashed red arrows. Poldip2 may interact with the neutrophil membrane fraction, with the PRR domain of p22^{phox} (based on comparison with Nox4-associated p22^{phox}) through its YccV like SH3 domain but also could develop through its DUF525 domain interaction with the region between the PX domain and the first SH3 of p47^{phox} (based on Alpha Fold modelling). (PB1 - phox and Bem1 domain, PPR proline rich region, PX - phox homology domains that bind to PtdIns-phosphates in the membrane, SH3 - Src homology 3 domains, TPR - tetricopeptide repeat domains, AD - activation domains, AIR - autoinhibitory region). (For interpretation of the references to color in this figure legend, the reader is referred to the Web version of this article.)

opposite effect on NADPH oxidase 4 was observed (here and in Ref. [6]). In the NADPH oxidase 4 complex, it was proposed that Poldip2 interacts with the PRR domain (155–160 amino acids) present in the soluble C-terminus part (121–193 amino acids) of p22^{phox} [6]. Because p22^{phox} is the same either in gp91^{phox} (Nox2) or Nox4 NADPH oxidases, we were expecting that Poldip2 similarly binds to gp91^{phox}-associated p22^{phox}. However, we observed that Poldip2 interacts only weakly with the neutrophil membrane fraction and in addition when Poldip2 was incubated with the MF prior to the addition of the cytosolic proteins, no decreased activity of NADPH oxidase 2 was measured. This raises the question of the role of p22^{phox} in Poldip2 binding when p22^{phox} is associated with gp91^{phox}. Several explanations could be proposed to explain this. The sequence homology between gp91^{phox} and Nox4 amino acid sequences is 39% which is significantly high to develop distinct interactions with p22^{phox} and in particular the C-terminus of p22^{phox} that could in turn alter the accessibility of Poldip2 to the PRR domain of gp91^{phox}-associated p22^{phox} [71]. Supporting this idea, it was shown that p22phox might adopt unique structural features when associated with Nox4 [72]. In addition, *in vivo*, post-translational modifications may change the interaction between Poldip2 and p22^{phox}. On one hand, databases such as NetPhos2 (http://www.cbs.dtu.dk/services/NetPhos-2.0) or Phosphositeplus (https://www.phosphosite.org/) indicate that Poldip2 possesses in its sequence several putative sites of phosphorylation, in particular T292 localized in the DUF525 domain. However, so far, no phosphorylation was reported for Poldip2 at this position, except post-UV irradiation in an ATR-dependent manner (DNA damage signaling kinase) at positions Ser147 and Ser150 [73]. Mass spectrometry analysis did not reveal any phosphorylation on Poldip2 produced in *P. pastoris*, which is known to be capable of post-translational modifications. However, our results showed that unphosphorylated recombinant Poldip2 was effective in up-regulating NADPH oxidase 4 suggesting that phosphorylation is not a major issue. Alternatively, the modified cysteine residue located in an internal channel observed recently in the structure of the human Poldip2 [10], could be a good candidate to influence, by redox conditions, structural changes that could modulate interactions between Poldip2 and p22^{phox}. On another hand, phosphorylation of p22^{phox} (Threonine 147) enhances NADPH oxidase 2 activity by promoting p47^{phox} binding [74] but no evidence of phosphorylation of the Nox4-associated p22^{phox} was found in the literature. Further studies should be addressed on the role of post-translational modifications of Poldip2 and Nox2-associated p22^{phox}. Finally, the weak Poldip2 interaction with the membrane could be also associated with the unspecific interaction of Poldip2 with membranes. In the YccV-like domain of Poldip2, the external face of C-ter α-helix contains positively charged residues allowing unspecific interaction with membrane bilayer phospholipids and therefore, could explain the lack of enzyme regulatory impact of Poldip2.

4.2. The p47^{phox} subunit, organizer subunit of NADPH oxidase2, as target of Poldip2

Even if we cannot exclude a similar interaction of Poldip2 with the p22^{phox} protein when associated with Nox2 or Nox4, this interaction was too weak to attribute it to the observed decrease of the NADPH oxidase 2 activity. Other explanations have to be considered.

Definitively, NADPH oxidases 2 and 4 function differently. On one hand, NADPH oxidase 4 requires only p22^{phox} to function and is a constitutively active enzyme. On the other hand, the functional gp91^{phox}/p22^{phox} depends on the translocation of cytosolic subunits p40^{phox}, p47^{phox}, p67^{phox}, and Rac. In the resting state, p47^{phox} can be found alone or interacting with p67^{phox} and p40^{phox} [75–77]. p47^{phox} and p67^{phox} interact through the C-terminal PRR domain of p47^{phox} and the SH3 domain of p67^{phox}. The p47^{phox}-p67^{phox} heterodimer is folded in such a way that the PX and SH3 domains of p47^{phox} are hidden and cannot interact with membrane phospholipids or with the C-ter PRR region of p22^{phox} [78]. Our results showed that Poldip2 interacts only with p47^{phox} since no obvious interaction with p67^{phox} or Rac could be detected. As shown in Fig. 6, once p47^{phox} binds to p67^{phox}, Poldip2 appears enabled to interact with p47^{phox}.

Since the YccV-like domain of the N-terminal region of Poldip2 is an SH3-like structure, we postulated that the strong interaction observed between Poldip2 and p47^{phox} may involve, similarly to p67^{phox}, the C-terminal PRR domain of p47^{phox}. Dot blot results with Poldip2 and the truncated form of p47^{phox}, where the PRR domain is absent, supported this hypothesis. However, we attempt to model the p47^{phox}-Poldip2 complex using the recent modeling facilities provided by AlphaFold2 (Fig. S7). The models propose that both proteins interact at the region between the PX domain and the bis-(SH3) domains of p47^{phox} and the DUF525 domain of Poldip2. This region of p47^{phox} is close to the bis-(SH3) domain that binds p22^{phox}. Further research could be undertaken to better identify the protein-protein interaction regions between Poldip2 and p47^{phox} but we could speculate that the interaction of Poldip2 to p47^{phox} could be different depending on the state of the protein (autoinhibited or activated) and could therefore interfere at different stages of NADPH oxidase and phagocyte activation.

In cells, the Poldip2-p47^{phox} association could have important impacts on the assembly/disassembly and consequently on the activity of the NADPH oxidase 2 complex. To the extent that p47^{phox} is found alone in the cytosol of immune cells (in a substantial amount [79]), Poldip2 could be a potential partner. During activation, 80–90% of p47^{phox} remains in the cytosol [80] and it has been shown that shortly after phagosome closure, p47^{phox} leaves the phagosome alone [81]. The interaction of Poldip2 with p47^{phox} could prevent further interaction of

p47^{phox} with the other NADPH oxidase proteins. Conversely, it could also be envisioned that the Poldip2-p47^{phox} dimer impacts the regulation of Nox4 activity by Poldip2. Altogether, this is a complex choreography of at least a trio of soluble proteins (p47^{phox}, p22^{phox}, and Poldip2) and a duo of membrane proteins (Nox4 and Nox2). Within a cell, the relative amounts of all these proteins (Nox2/p22^{phox} *versus* Nox4/p22^{phox}; p47^{phox} *versus* Poldip2) can vary considerably from one cell type to another or throughout the life of the cell. It is conceivable that at a given time, p47^{phox} might be absent or in very strong minority. It was shown that i*n vitro* p47^{phox} is not dispensable to the Nox2 activity, since in its absence, superoxide production (40% of the activity) has been measured whether p67^{phox} and Rac were in excess [82,83]. The variability of their relative amount of the different proteins can be of importance for the regulation of both isoforms. Based on our hypothesis, cells with a low concentration of p47^{phox} should have a strongly inhibited Nox2 in the presence of Poldip2.

4.3. Role of Poldip2 in phagocyte cells

This question is in principle relevant in cells where Poldip2 together with PCNA could orchestrate the biological regulation of ROS production and other complex biological processes. It was shown recently that PCNA controls neutrophil survival through association with p47^{phox} at the level of its phox homology (PX) domain [84]. Since Poldip2 plays the role of a chaperone protein that coordinates the interaction of polymerases with PCNA [18], Poldip2 might be a third partner in the regulation between PCNA and p47^{phox} in the regulation of Nox2 activity in cells such as monocytes or macrophages. No studies have been performed in such cells yet.

Also, it is surprising to note that, as described in the literature, neutrophils produce much more ROS than other immune system cells such as monocytes and macrophages [85–88]. However, gp91^{phox}/p22^{phox} proteins are expressed at a similar level in neutrophils and macrophages (based on the signal corresponding to p22^{phox}; 1:1 with gp91^{phox}). Thus, the high levels of gp91^{phox}/p22^{phox} expressed in macrophages are not consistent with their low levels of ROS production compared to neutrophils. The presence of endogenous Poldip2 especially in macrophages, but not in circulating neutrophils, could have a negative regulatory effect on the NADPH oxidase 2 activity in these cells. This means that Poldip2, by differentially regulating NADPH oxidases 2 and 4, acts as a switch of the ROS source at a given time by its ability to increase the activity of NADPH oxidase 4 and at the same time, decrease the activity of NADPH oxidase 2. It is also very interesting to consider the nature of the ROS since Nox2 produces superoxide ($O^{\bullet-}_2$) while Nox4 generates hydrogen peroxide (H_2O_2). A regulation by Poldip2 could thus modify the relative amount of ROS produced (H_20_2 *versus* $O_2^{\bullet-}$). This could be particularly interesting from a therapeutic point of view if it is possible to target a decrease in $O_2^{\bullet-}$ production while increasing H_2O_2 production. This could be also of importance in the regulation of intracellular ROS in macrophages or monocytes where NADPH oxidase 4 has been identified and proposed to be involved in macrophage death [89]. We show here that circulating resting neutrophils do not express Poldip2, but the situation might be different at other stages of cell maturation of neutrophils such as during the hematopoietic differentiation where Nox4 is the isoform responsible for the ROS generation [90]. Consistent with this hypothesis, Poldip2 was identified in myeloid neutrophils in a very recent work showing a role of Poldip2 in neutrophil recruitment [25]. Given the paucity of studies of Poldip2 on these cells and the observations obtained in this work on its effect on Nox2, it would be particularly interesting to further investigate the involvement of Poldip2 at the cellular level of the innate immune system.

To our knowledge, the present study is the first to show a down-regulation of phagocyte NADPH oxidase by a cytosolic protein. Poldip2 acts as a cytosolic partner trapping free p47^{phox} prior its assembly to the oxidase complex. However further studies should be addressed to decipher the role of post-translational modifications of Poldip2, Nox2/p22^{phox}, and p47^{phox} including phosphorylation (autoinhibited or activated) or redox (cysteine) signaling events, that occur during neutrophil maturation or activation. This should help to understand more-in-depth the mechanisms that control Poldip2-p22^{phox} and Poldip2-p47^{phox} association. New insights should be brought to better understand the mechanism of the cross-regulation between Nox2/p22^{phox} and Nox4/p22^{phox} and their consequences considering the fact that they lead to different reaction products (H_2O_2 versus $O_2^{\bullet-}$), they function differently (constitutive versus activatable; different Vmax) and might be subject to different post-translational modifications.

Author contributions

A.B. performed research; R.A.L. contributed for NOX4 experiments; S.A. performed control dot blots, analysis and structure modeling; P.M.-C.D. contributed to monocyte and macrophage experiments; T.B. contributed to neutrophil and cytosolic protein purifications; C.D. supervised HEK cell experiments; J.W. performed the IR measurements; P.M.-C.D., T.B. and C.D. contributed to scientific discussions; A.B. and L.B. designed research and wrote the paper. All authors commented on the article.

Declaration of competing interest

The authors declare that they have no known competing financial interests or personal relationships that could have appeared to influence the work reported in this paper.

Acknowledgements

SRCD measurements on DISCO beamline at Synchrotron SOLEIL were performed under the proposal 20211318. Authors want to acknowledge Dr. B. Lassègue for providing with rat Poldip2 containing plasmid. We are very grateful to L. Saigo and D. Cornu at the SICaPS platform (Service d'Identification et de Caractérisation des Protéines par Spectrométrie de masse, Gif/Yvette, France) for the mass spectrometry analysis. S. A. salary was granted by the Palm Labex Paris Saclay and A. B. salary by the French Ministère de l'enseignement supérieur et de la recherche (MESR).

Appendix A. Supplementary data

Supplementary data to this article can be found online at https://doi.org/10.1016/j.freeradbiomed.2023.02.019.

References

[1] X. Cheng, T. Kanki, A. Fukuoh, K. Ohgaki, R. Takeya, Y. Aoki, N. Hamasaki, D. Kang, PDIP38 associates with proteins constituting the mitochondrial DNA nucleoid, J. Biochem. 138 (6) (2005) 673–678.
[2] E. Klaile, M.M. Muller, C. Kannicht, W. Otto, B.B. Singer, W. Reutter, B. Obrink, L. Lucka, The cell adhesion receptor carcinoembryonic antigen-related cell adhesion molecule 1 regulates nucleocytoplasmic trafficking of DNA polymerase delta-interacting protein 38, J. Biol. Chem. 282 (36) (2007) 26629–26640.
[3] L. Liu, E.M. Rodriguez-Belmonte, N. Mazloum, B. Xie, M.Y.W.T. Lee, Identification of a novel protein, PDIP38, that interacts with the p50 subunit of DNA polymerase delta and proliferating cell nuclear antigen, J. Biol. Chem. 278 (12) (2003) 10041–10047.
[4] B. Xie, H. Li, Q. Wang, S. Xie, A. Rahmeh, W. Dai, M.Y. Lee, Further characterization of human DNA polymerase delta interacting protein 38, J. Biol. Chem. 280 (23) (2005) 22375–22384.
[5] N. Arakaki, T. Nishihama, A. Kohda, H. Owaki, Y. Kuramoto, R. Abe, T. Kita, M. Suenaga, T. Himeda, M. Kuwajima, H. Shibata, T. Higuti, Regulation of mitochondrial morphology and cell survival by Mitogenin I and mitochondrial single-stranded DNA binding protein, Biochim. Biophys. Acta 1760 (9) (2006) 1364–1372.
[6] A.N. Lyle, N.N. Deshpande, Y. Taniyama, B. Seidel-Rogol, L. Pounkova, P.F. Du, C. Papaharalambus, B. Lassegue, K.K. Griendling, Poldip2, a novel regulator of Nox4 and cytoskeletal integrity in vascular smooth muscle cells, Circ. Res. 105 (3)

(2009) 249 U116.
[7] D.O. Cicero, G.M. Contessa, T.A. Pertinhez, M. Gallo, A.M. Katsuyama, M. Paci, C.S. Farah, A. Spisni, Solution structure of ApaG from Xanthomonas axonopodis pv. citri reveals a fibronectin-3 fold, Proteins: Struct., Funct., Bioinf. 67 (2) (2007) 490–500.
[8] T.A. Guilliam, L.J. Bailey, N.C. Brissett, A.J. Doherty, PolDIP2 interacts with human PrimPol and enhances its DNA polymerase activities, Nucleic Acids Res. 44 (7) (2016) 3317–3329.
[9] M.S. Hernandes, B. Lassegue, K.K. Griendling, Polymerase delta-interacting protein 2: a multifunctional protein, J. Cardiovasc. Pharmacol. 69 (6) (2017) 335–342.
[10] A.A. Kulik, K.K. Maruszczak, D.C. Thomas, N.L.A. Nabi, M. Carr, R.J. Bingham, C.D.O. Cooper, Crystal structure and molecular dynamics of human POLDIP2, a multifaceted adaptor protein in metabolism and genome stability, Protein Sci 30 (2021) 1196–1209.
[11] P.R. Strack, E.J. Brodie, H.M. Zhan, V.J. Schuenemann, L.J. Valente, T. Saiyed, B.R. Lowth, L.M. Angley, M.A. Perugini, K. Zeth, K.N. Truscott, D.A. Dougan, Polymerase delta-interacting protein 38 (PDIP38) modulates the stability and activity of the mitochondrial AAA plus protease CLPXP, Communications Biology 3 (1) (2020).
[12] E. d'Alencon, A. Taghbalout, C. Bristow, R. Kern, R. Aflalo, M. Kohiyama, Isolation of a new hemimethylated DNA binding protein which regulates dnaA gene expression, J. Bacteriol. 185 (9) (2003) 2967–2971.
[13] M. Nakamura, A. Eguchi, M. Inohana, R. Nagahara, H. Murayama, M. Kawashima, S. Mizukami, M. Koyanagi, S.M. Hayashi, R.R. Maronpot, M. Shibutani, T. Yoshida, Differential impacts of mineralocorticoid receptor antagonist potassium canrenoate on liver and renal changes in high fat diet-mediated early hepatocarcinogenesis model rats, J. Toxicol. Sci. 43 (10) (2018) 611–621.
[14] T.R. Shimuta, K. Nakano, Y. Yamaguchi, S. Ozaki, K. Fujimitsu, C. Matsunaga, K. Noguchi, A. Emoto, T. Katayama, Novel heat shock protein HspQ stimulates the degradation of mutant DnaA protein in Escherichia coli, Gene Cell. 9 (12) (2004) 1151–1166.
[15] G.P. Ilyin, M. Rialland, C. Pigeon, C. Guguen-Guillouzo, cDNA cloning and expression analysis of new members of the mammalian F-box protein family, Genomics 67 (1) (2000) 40–47.
[16] J.T. Winston, D.M. Koepp, C. Zhu, S.J. Elledge, J.W. Harper, A family of mammalian F-box proteins, Curr. Biol. 9 (20) (1999) 1180–1182.
[17] R.M. Monaghan, A.J. Whitmarsh, Mitochondrial proteins moonlighting in the nucleus, Trends Biochem. Sci. 40 (12) (2015) 728–735.
[18] G. Maga, E. Crespan, E. Markkanen, R. Imhof, A. Furrer, G. Villani, U. Hubscher, B. van Loon, DNA polymerase delta-interacting protein 2 is a processivity factor for DNA polymerase lambda during 8-oxo-7,8-dihydroguanine bypass, Proc. Natl. Acad. Sci. U. S. A. 110 (47) (2013) 18850–18855.
[19] A. Tissier, R. Janel-Bintz, S. Coulon, E. Klaile, P. Kannouche, R.P. Fuchs, A.M. Cordonnier, Crosstalk between replicative and translesional DNA polymerases: PDIP38 interacts directly with Poleta, DNA Repair 9 (8) (2010) 922–928.
[20] B.J. Floyd, E.M. Wilkerson, M.T. Veling, C.E. Minogue, C. Xia, E.T. Beebe, R.L. Wrobel, H. Cho, L.S. Kremer, C.L. Alston, K.A. Gromek, B.K. Dolan, A. Ulbrich, J.A. Stefely, S.L. Bohl, K.M. Werner, A. Jochem, M.S. Westphall, J.W. Rensvold, R.W. Taylor, H. Prokisch, J.P. Kim, J.J. Coon, D.J. Pagliarini, Mitochondrial protein interaction mapping identifies regulators of respiratory chain function, Mol Cell 63 (4) (2016) 621–632.
[21] U. Stelzl, U. Worm, M. Lalowski, C. Haenig, F.H. Brembeck, H. Goehler, M. Stroedicke, M. Zenkner, A. Schoenherr, S. Koeppen, J. Timm, S. Mintzlaff, C. Abraham, N. Bock, S. Kietzmann, A. Goedde, E. Toksoz, A. Droege, S. Krobitsch, B. Korn, W. Birchmeier, H. Lehrach, E.E. Wanker, A human protein-protein interaction network: a resource for annotating the proteome, Cell 122 (6) (2005) 957–968.
[22] S.R. Datla, D.J. McGrail, S. Vukelic, L.P. Huff, A.N. Lyle, L. Pounkova, M. Lee, B. Seidel-Rogol, M.K. Khalil, L.L. Hilenski, L.S. Terada, M.R. Dawson, B. Lassegue, K.K. Griendling, Poldip2 controls vascular smooth muscle cell migration by regulating focal adhesion turnover and force polarization, Am. J. Physiol. Heart Circ. Physiol. 307 (7) (2014) H945–H957.
[23] S. Vukelic, Q. Xu, B. Seidel-Rogol, E.A. Faidley, A.E. Dikalova, L.L. Hilenski, U. Jorde, L.B. Poole, B. Lassegue, G. Zhang, K.K. Griendling, NOX4 (NADPH oxidase 4) and Poldip2 (polymerase delta-interacting protein 2) induce filamentous actin oxidation and promote its interaction with vinculin during integrin-mediated cell adhesion, Arterioscler. Thromb. Vasc. Biol. 38 (10) (2018) 2423–2434.
[24] S. Matsushima, D. Zablocki, H. Tsutsui, J. Sadoshima, Poldip2 negatively regulates matrix synthesis at focal adhesions, J. Mol. Cell. Cardiol. 94 (2016) 10–12.
[25] Z. Ou, E. Dolmatova, R. Mandavilli, H. Qu, G. Gafford, T. White, A. Valdivia, B. Lassegue, M.S. Hernandes, K.K. Griendling, Myeloid Poldip2 contributes to the development of pulmonary inflammation by regulating neutrophil adhesion in a murine model of acute respiratory distress syndrome, J. Am. Heart Assoc. 11 (10) (2022) e025181.
[26] K. Kasho, L. Krasauskas, V. Smirnovas, G. Stojkovic, L.A. Morozova-Roche, S. Wanrooij, Human polymerase delta-interacting protein 2 (PolDIP2) inhibits the formation of human Tau oligomers and fibrils, Int. J. Mol. Sci. 22 (11) (2021).
[27] M.U. Moreno, I. Gallego, B. Lopez, A. Gonzalez, A. Fortuno, G. San Jose, F. Valencia, J.J. Gomez-Doblas, E. de Teresa, A.M. Shah, J. Diez, G. Zalba, Decreased Nox4 levels in the myocardium of patients with aortic valve stenosis, Clin. Sci. (Lond.) 125 (6) (2013) 291–300.
[28] J.Y.K. Chan, P.H.Y. Poon, Y. Zhang, C.W.K. Ng, W.Y. Piao, M. Ma, K.Y. Yip, A.B.W. Chan, V.W.Y. Lui, Case Report: exome sequencing reveals recurrent RETSAT mutations and a loss-of-function POLDIP2 mutation in a rare undifferentiated tongue sarcoma, F1000Res 7 (2018) 499.
[29] Y.C. Chen, C.C. Kuo, C.F. Chian, C. Tzao, S.Y. Chang, Y.L. Shih, Y.W. Lin, M.H. Yu, H.Y. Su, Knockdown of POLDIP2 suppresses tumor growth and invasion capacity and is linked to unfavorable transformation ability and metastatic feature in non-small cell lung cancer, Exp. Cell Res. 368 (1) (2018) 42–49.
[30] C.F. Chian, Y.T. Hwang, H.J. Terng, S.C. Lee, T.Y. Chao, H. Chang, C.L. Ho, Y.Y. Wu, W.C. Perng, Panels of tumor-derived RNA markers in peripheral blood of patients with non-small cell lung cancer: their dependence on age, gender and clinical stages, Oncotarget 7 (31) (2016) 50582–50595.
[31] O.V. Grinchuk, E. Motakis, V.A. Kuznetsov, Complex sense-antisense architecture of TNFAIP1/POLDIP2 on 17q11.2 represents a novel transcriptional structural-functional gene module involved in breast cancer progression, BMC Genom. 11 (Suppl 1) (2010) S9.
[32] A. Vinayagam, U. Stelzl, R. Foulle, S. Plassmann, M. Zenkner, J. Timm, H.E. Assmus, M.A. Andrade-Navarro, E.E. Wanker, A directed protein interaction network for investigating intracellular signal transduction, Sci. Signal. 4 (189) (2011) rs8.
[33] L. Horbach, M. Sinigaglia, C.A. Da Silva, D.B. Olguins, L.J. Gregianin, A.L. Brunetto, A.T. Brunetto, R. Roesler, C.B. De Farias, Gene expression changes associated with chemotherapy resistance in Ewing sarcoma cells, Mol Clin Oncol 8 (6) (2018) 719–724.
[34] F. Paredes, K. Sheldon, B. Lassegue, H.C. Williams, E.A. Faidley, G.A. Benavides, G. Torres, F. Sanhueza-Olivares, S.M. Yeligar, K.K. Griendling, V. Darley-Usmar, A. San Martin, Poldip2 is an oxygen-sensitive protein that controls PDH and alphaKGDH lipoylation and activation to support metabolic adaptation in hypoxia and cancer, Proc. Natl. Acad. Sci. U. S. A. 115 (8) (2018) 1789–1794.
[35] S.J. Forrester, Q. Xu, D.S. Kikuchi, D. Okwan-Duodu, A.C. Campos, E.A. Faidley, G. Zhang, B. Lassegue, R.T. Sadikot, K.K. Griendling, M.S. Hernandes, Poldip2 deficiency protects against lung edema and vascular inflammation in a model of acute respiratory distress syndrome, Clin. Sci. (Lond.) 133 (2) (2019) 321–334.
[36] L.N. Eidson, Q.Z. Gao, H.Y. Qu, D.S. Kikuchi, A.C.P. Campos, E.A. Faidley, Y.Y. Sun, C.Y. Kuan, R.L. Pagano, B. Lassegue, M.G. Tansey, K.K. Griendling, M.S. Hernandes, Poldip2 controls leukocyte infiltration into the ischemic brain by regulating focal adhesion kinase-mediated VCAM-1 induction, Sci. Rep. 11 (1) (2021).
[37] M.S. Hernandes, B. Lassegue, L.L. Hilenski, J. Adams, N. Gao, C.Y. Kuan, Y.Y. Sun, L. Cheng, D.S. Kikuchi, M. Yepes, K.K. Griendling, Polymerase delta-interacting protein 2 deficiency protects against blood-brain barrier permeability in the ischemic brain, J. Neuroinflammation 15 (1) (2018) 45.
[38] Y. Kim, H. Park, J. Nah, S. Moon, W. Lee, S.H. Hong, T.I. Kam, Y.K. Jung, Essential role of POLDIP2 in Tau aggregation and neurotoxicity via autophagy/proteasome inhibition, Biochem. Biophys. Res. Commun. 462 (2) (2015) 112–118.
[39] C.S. Lin, S.H. Lee, H.S. Huang, Y.S. Chen, M.C. Ma, H2O2 generated by NADPH oxidase 4 contributes to transient receptor potential vanilloid 1 channel-mediated mechanosensation in the rat kidney, Am. J. Physiol. Ren. Physiol. 309 (4) (2015) F369–F376.
[40] H. Dosoki, A. Stegemann, M. Taha, H. Schnittler, T.A. Luger, K. Schroder, J.H. Distler, C. Kerkhoff, M. Bohm, Targeting of NADPH oxidase in vitro and in vivo suppresses fibroblast activation and experimental skin fibrosis, Exp. Dermatol. 26 (1) (2016) 73–81.
[41] N. Manickam, M. Patel, K.K. Griendling, Y. Gorin, J.L. Barnes, RhoA/Rho kinase mediates TGF-beta1-induced kidney myofibroblast activation through Poldip2/Nox4-derived reactive oxygen species, Am. J. Physiol. Ren. Physiol. 307 (2) (2014) F159–F171.
[42] K. Bedard, K.H. Krause, The NOX family of ROS-generating NADPH oxidases: physiology and pathophysiology, Physiol. Rev. 87 (1) (2007) 245–313.
[43] Y. Nisimoto, B.A. Diebold, D. Cosentino-Gomes, J.D. Lambeth, Nox4: a hydrogen peroxide-generating oxygen sensor, Biochemistry 53 (31) (2014) 5111–5120.
[44] A. Shiose, J. Kuroda, K. Tsuruya, M. Hirai, H. Hirakata, S. Naito, M. Hattori, Y. Sakaki, H. Sumimoto, A novel superoxide-producing NAD(P)H oxidase in kidney, J. Biol. Chem. 276 (2) (2001) 1417–1423.
[45] L. Serrander, L. Cartier, K. Bedard, B. Banfi, B. Lardy, O. Plastre, A. Sienkiewicz, L. Forro, W. Schlegel, K.H. Krause, NOX4 activity is determined by mRNA levels and reveals a unique pattern of ROS generation, Biochem. J. 406 (2007) 105–114.
[46] S. Furukawa, T. Fujita, M. Shimabukuro, M. Iwaki, Y. Yamada, Y. Nakajima, O. Nakayama, M. Makishima, M. Matsuda, I. Shimomura, Increased oxidative stress in obesity and its impact on metabolic syndrome, J. Clin. Invest. 114 (12) (2004) 1752–1761.
[47] N.N.C. Tam, Y. Gao, Y.K. Leung, S.M. Ho, Androgenic regulation of oxidative stress in the rat prostate - involvement of NAD(P)H oxidases and antioxidant defense machinery during prostatic involution and regrowth, Am. J. Pathol. 163 (6) (2003) 2513–2522.
[48] G.J. Cheng, Z.H. Cao, X.X. Xu, E.G. Van Meir, J.D. Lambeth, Homologs of gp91phox: cloning and tissue expression of Nox3, Nox4, and Nox5, Gene 269 (1–2) (2001) 131–140.
[49] J.K. Bendall, R. Rinze, D. Adlam, A.L. Tatham, J. de Bono, K.M. Channon, Endothelial Nox2 overexpression potentiates vascular oxidative stress and hemodynamic response to angiotensin II - studies in endothelial-targeted Nox2 transgenic mice, Circ. Res. 100 (7) (2007) 1016–1025.
[50] K.K. Griendling, Novel NAD(P)H oxidases in the cardiovascular system, Heart 90 (5) (2004) 491–493.
[51] J.D. Van Buul, M. Fernandez-Borja, E.C. Anthony, P.L. Hordijk, Expression and localization of NOX2 and NOX4 in primary human endothelial cells, Antioxidants Redox Signal. 7 (3–4) (2005) 308–317.
[52] L. Li, E.Y. Lai, Z. Luo, G. Solis, K.K. Griendling, W.R. Taylor, P.A. Jose, A.

Wellstein, W.J. Welch, C.S. Wilcox, Superoxide and hydrogen peroxide counterregulate myogenic contractions in renal afferent arterioles from a mouse model of chronic kidney disease, Kidney Int. 92 (3) (2017) 625–633.
[53] L. Li, E.Y. Lai, Z. Luo, G. Solis, M. Mendonca, K.K. Griendling, A. Wellstein, W.J. Welch, C.S. Wilcox, High salt enhances reactive oxygen species and angiotensin II contractions of glomerular afferent arterioles from mice with reduced renal mass, Hypertension 72 (5) (2018) 1208–1216.
[54] T. Bizouarn, H. Souabni, X. Serfaty, A. Bouraoui, R. Masoud, G. Karimi, C. Houee-Levin, L. Baciou, A close-up view of the impact of arachidonic acid on the phagocyte NADPH oxidase, Nadph Oxidases: Methods and Protocols 1982 (2019) 75–101.
[55] X. Serfaty, P. Lefrancois, C. Houee-Levin, S. Arbault, L. Baciou, T. Bizouarn, Impacts of vesicular environment on Nox2 activity measurements in vitro, Biochim. Biophys. Acta Gen. Subj. 1865 (1) (2021) 129767.
[56] T. Schwede, J. Kopp, N. Guex, M.C. Peitsch, SWISS-MODEL: an automated protein homology-modeling server, Nucleic Acids Res. 31 (13) (2003) 3381–3385.
[57] M. Mirdita, K. Schutze, Y. Moriwaki, L. Heo, S. Ovchinnikov, M. Steinegger, ColabFold: making protein folding accessible to all, Nat. Methods 19 (6) (2022) 679–682.
[58] E. Goormaghtigh, J.M. Ruysschaert, V. Raussens, Evaluation of the information content in infrared spectra for protein secondary structure determination, Biophys. J. 90 (8) (2006) 2946–2957.
[59] T.C. Krzysiak, B.B. Chen, T. Lear, R.K. Mallampalli, A.M. Gronenborn, Crystal structure and interaction studies of the human FBxo3 ApaG domain, FEBS J. 283 (11) (2016) 2091–2101.
[60] J. Jumper, R. Evans, A. Pritzel, T. Green, M. Figurnov, O. Ronneberger, K. Tunyasuvunakool, R. Bates, A. Zidek, A. Potapenko, A. Bridgland, C. Meyer, S.A.A. Kohl, A.J. Ballard, A. Cowie, B. Romera-Paredes, S. Nikolov, R. Jain, J. Adler, T. Back, S. Petersen, D. Reiman, E. Clancy, M. Zielinski, M. Steinegger, M. Pacholska, T. Berghammer, S. Bodenstein, D. Silver, O. Vinyals, A.W. Senior, K. Kavukcuoglu, P. Kohli, D. Hassabis, Highly accurate protein structure prediction with AlphaFold, Nature 596 (7873) (2021) 583–+.
[61] J. Kuroda, T. Ago, S. Matsushima, P.Y. Zhai, M.D. Schneider, J. Sadoshima, NADPH oxidase 4 (Nox4) is a major source of oxidative stress in the failing heart, Proc. Natl. Acad. Sci. U. S. A. 107 (35) (2010) 15565–15570.
[62] H. Souabni, P. Machillot, L. Baciou, Contribution of lipid environment to NADPH oxidase activity: influence of sterol, Biochimie 107 Pt A (2014) 33–42.
[63] M.C. Dagher, E. Pick, Opening the black box: lessons from cell-free systems on the phagocyte NADPH-oxidase, Biochimie 89 (9) (2007) 1123–1132.
[64] E. Pick, Cell-free NADPH oxidase activation assays: a triumph of reductionism, Methods Mol. Biol. 2087 (2020) 325–411.
[65] T. Bizouarn, G. Karimi, R. Masoud, H. Souabni, P. Machillot, X. Serfaty, F. Wien, M. Refregiers, C. Houee-Levin, L. Baciou, Exploring the arachidonic acid-induced structural changes in phagocyte NADPH oxidase p47(phox) and p67(phox) via thiol accessibility and SRCD spectroscopy, FEBS J. 283 (15) (2016) 2896–2910.
[66] K. Kami, R. Takeya, H. Sumimoto, D. Kohda, Diverse recognition of non-PxxP peptide ligands by the SH3 domains from p67(phox), Grb2 and Pex13p, EMBO J. 21 (16) (2002) 4268–4276.
[67] K. Lapouge, S.J.M. Smith, P.A. Walker, S.J. Gamblin, S.J. Smerdon, K. Rittinger, Structure of the TPR domain of p67(phox) in complex with Rac center dot GTP, Mol. Cell 6 (4) (2000) 899–907.
[68] G. Karimi, C. Houee Levin, M.C. Dagher, L. Baciou, T. Bizouarn, Assembly of phagocyte NADPH oxidase: a concerted binding process? Biochim. Biophys. Acta 1840 (11) (2014) 3277–3283.
[69] K. Hata, K. Takeshige, H. Sumimoto, Roles for proline-rich regions of p47phox and p67phox in the phagocyte NADPH oxidase activation in vitro, Biochem. Biophys. Res. Commun. 241 (2) (1997) 226–231.
[70] T.L. Leto, A.G. Adams, I. de Mendez, Assembly of the phagocyte NADPH oxidase: binding of Src homology 3 domains to proline-rich targets, Proc. Natl. Acad. Sci. U. S. A. 91 (22) (1994) 10650–10654.
[71] I. deMendez, A. Abo, T. Leto, Down-regulation of a phagocyte host defense system, the NADPH oxidase, by PAK2, Mol. Biol. Cell 8 (1997) 772 772.
[72] K. von Lohneysen, D. Noack, A.J. Jesaitis, M.C. Dinauer, U.G. Knaus, Mutational analysis reveals distinct features of the Nox4-p22 phox complex, J. Biol. Chem. 283 (50) (2008) 35273–35282.
[73] C. Peddu, S. Zhang, H. Zhao, A. Wong, E.Y.C. Lee, M. Lee, Z. Zhang, Phosphorylation alters the properties of pol eta: implications for translesion synthesis, iScience 6 (2018) 52–67.
[74] E.M. Lewis, S. Sergeant, B. Ledford, N. Stull, M.C. Dinauer, L.C. McPhail, Phosphorylation of p22phox on threonine 147 enhances NADPH oxidase activity by promoting p47phox binding, J. Biol. Chem. 285 (5) (2009) 2959–2967.
[75] K. Lapouge, S.J. Smith, Y. Groemping, K. Rittinger, Architecture of the p40-p47-p67phox complex in the resting state of the NADPH oxidase. A central role for p67phox, J. Biol. Chem. 277 (12) (2002) 10121–10128.
[76] J.W. Park, J.E. Benna, K.E. Scott, B.L. Christensen, S.J. Chanock, B.M. Babior, Isolation of a complex of respiratory burst oxidase components from resting neutrophil cytosol, Biochemistry 33 (10) (1994) 2907–2911.
[77] C.S. Ziegler, L. Bouchab, M. Tramier, D. Durand, F. Fieschi, S. Dupre-Crochet, F. Merola, O. Nusse, M. Erard, Quantitative live-cell imaging and 3D modeling reveal critical functional features in the cytosolic complex of phagocyte NADPH oxidase, J. Biol. Chem. 294 (11) (2019) 3824–3836.
[78] Y. Groemping, K. Lapouge, S.J. Smerdon, K. Rittinger, Molecular basis of phosphorylation-induced activation of the NADPH oxidase, Cell 113 (3) (2003) 343–355.
[79] P.G. Heyworth, B.P. Bohl, G.M. Bokoch, J.T. Curnutte, Rac translocates independently of the neutrophil NADPH oxidase components p47phox and p67phox. Evidence for its interaction with flavocytochrome b558, J. Biol. Chem. 269 (49) (1994) 30749–30752.
[80] R.A. Clark, B.D. Volpp, K.G. Leidal, W.M. Nauseef, Two cytosolic components of the human neutrophil respiratory burst oxidase translocate to the plasma membrane during cell activation, J. Clin. Invest. 85 (3) (1990) 714–721.
[81] M.C. Faure, J.C. Sulpice, M. Delattre, M. Lavielle, M. Prigent, M.H. Cuif, C. Melchior, E. Tschirhart, O. Nusse, S. Dupre-Crochet, The recruitment of p47(phox) and Rac2G12V at the phagosome is transient and phosphatidylserine dependent, Biol. Cell. 105 (11) (2013) 501–518.
[82] V. Koshkin, O. Lotan, E. Pick, The cytosolic component p47(phox) is not a sine qua non participant in the activation of NADPH oxidase but is required for optimal superoxide production, J. Biol. Chem. 271 (48) (1996) 30326–30329.
[83] J.L. Freeman, J.D. Lambeth, NADPH oxidase activity is independent of p47phox in vitro, J. Biol. Chem. 271 (37) (1996) 22578–22582.
[84] D. Ohayon, A. De Chiara, P.M.C. Dang, N. Thieblemont, S. Chatfield, V. Marzaioli, S.S. Burgener, J. Mocek, C. Candalh, C. Pintard, P. Tacnet-Delorme, G. Renault, I. Lagoutte, M. Favier, F. Walker, M. Hurtado-Nedelec, D. Desplancq, E. Weiss, C. Benarafa, D. Housset, J.C. Marie, P. Frachet, J. El-Benna, V. Witko-Sarsat, Cytosolic PCNA interacts with p47phox and controls NADPH oxidase NOX2 activation in neutrophils, J. Exp. Med. 216 (11) (2019) 2669–2687.
[85] M.K. Cathcart, Regulation of superoxide anion production by NADPH oxidase in monocytes/macrophages - contributions to atherosclerosis, Arterioscler. Thromb. Vasc. Biol. 24 (1) (2004) 23–28.
[86] M.L. Devalon, G.R. Elliott, W.E. Regelmann, Oxidative response of human-neutrophils, monocytes, and alveolar macrophages induced by unopsonized surface-adherent staphylococcus-aureus, Infect. Immun. 55 (10) (1987) 2398–2403.
[87] N.E. Gomes, M.K.C. Brunialti, M.E. Mendes, M. Freudenberg, C. Galanos, R. Salomao, Lipopolysaccharide-induced expression of cell surface receptors and cell activation of neutrophils and monocytes in whole human blood, Braz. J. Med. Biol. Res. 43 (9) (2010) 853–859.
[88] V. Ponath, B. Kaina, Death of monocytes through oxidative burst of macrophages and neutrophils: killing in trans, PLoS One 12 (1) (2017).
[89] C.F. Lee, M. Qiao, K. Schroder, Q. Zhao, R. Asmis, Nox4 is a novel inducible source of reactive oxygen species in monocytes and macrophages and mediates oxidized low density lipoprotein-induced macrophage death, Circ. Res. 106 (9) (2010) 1489–1497.
[90] J. Brault, B. Vigne, M. Meunier, S. Beaumel, M. Mollin, S. Park, M.J. Stasia, NOX4 is the main NADPH oxidase involved in the early stages of hematopoietic differentiation from human induced pluripotent stem cells, Free Radic. Biol. Med. 146 (2020) 107–118.